
Masters Theses

Student Theses and Dissertations

1965

Study of deformation of non-oscillating droplets in liquid media

Arun Kumar Agrawal

Follow this and additional works at: https://scholarsmine.mst.edu/masters_theses



Part of the [Chemical Engineering Commons](#)

Department:

Recommended Citation

Agrawal, Arun Kumar, "Study of deformation of non-oscillating droplets in liquid media" (1965). *Masters Theses*. 6969.

https://scholarsmine.mst.edu/masters_theses/6969

This thesis is brought to you by Scholars' Mine, a service of the Missouri S&T Library and Learning Resources. This work is protected by U. S. Copyright Law. Unauthorized use including reproduction for redistribution requires the permission of the copyright holder. For more information, please contact scholarsmine@mst.edu.

STUDY OF DEFORMATION
OF NON-OSCILLATING DROPLETS IN LIQUID MEDIA

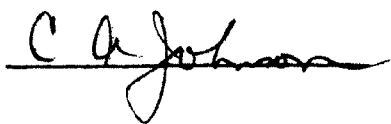
by
ARUN KUMAR AGRAWAL

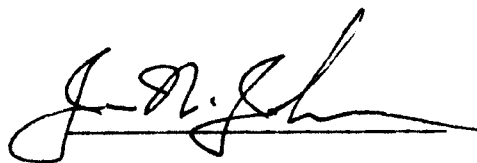
A
THESIS

submitted to the faculty of the
UNIVERSITY OF MISSOURI AT ROLLA
in partial fulfillment of the requirements for the
Degree of
MASTER OF SCIENCE IN CHEMICAL ENGINEERING
Rolla, Missouri
1965

Approved by

 (advisor)







ABSTRACT

The object of this investigation was to find a method for predicting the deformation of non-oscillating liquid droplets which are moving in liquid media, from a knowledge of droplet size and the physical properties of the continuous and dispersed phase systems. The deformation of thirteen liquid-liquid systems was experimentally studied in this investigation, and these systems are listed below, the dispersed phase given first:

1. Nitrobenzene in water
2. Carbon tetrachloride in water
3. Water in methyl isobutyl ketone
4. Water in hexane
5. Bromobenzene in water
6. Aniline in water
7. Nitrobenzene in glycol
8. Glycol in hexane
9. Water in corn oil
10. Glycol in benzene
11. Water in benzene
12. Benzyl alcohol in hexane
13. Glycol in methyl isobutyl ketone

Data for the last three systems could not be obtained for experimental reasons.

The existing empirical graphical correlation of Harmathy predicted the drop deformation (in the form of eccentricity) of the systems studied in this investigation and in the literature with an average absolute deviation of 13.6 percent. Five new empirical correlations were obtained for predicting drop deformation as eccentricity. The following two correlations have been recommended for use:

$$E = 1.0 + 0.123E\ddot{o}$$

$$E = 1.0 + 0.091We^{0.95}$$

where,

E = the droplet eccentricity

$E\ddot{o}$ = Eötvös number

We = Weber number

The average absolute deviation of the calculated eccentricities from observed eccentricities for the ten systems used in this study and 39 systems reported in the literature are 7.8 and 6.2 percent for the above two correlations, respectively.

TABLE OF CONTENTS

	<u>Page</u>
ABSTRACT	i
TABLE OF CONTENTS	iii
LIST OF FIGURES	vi
LIST OF TABLES	viii
I. INTRODUCTION	1
II. LITERATURE REVIEW	3
A. Introduction to Drop Mechanics	3
B. Mechanics of Rigid Particles	4
C. Mechanics of Droplets in Liquid-Liquid Systems	6
1. Formation of Liquid Droplets	8
2. Terminal Velocity	8
3. Peak Velocity	14
4. Wall Effect on Velocity	15
5. Drag Coefficient	16
6. Circulation within Droplets	20
7. Shape	21
8. Oscillation	33
9. Maximum Drop Size	35
10. Effect of Shape on Mass Transfer	35
III. EXPERIMENTAL	40
A. Object of Investigation	40

	<u>Page</u>
B. Materials	40
C. Systems	40
D. Physical Properties	42
E. Apparatus	43
F. Experimental Procedure	48
G. Sample Calculations	50
H. Results	52
IV. DISCUSSION	53
A. Data from Literature	53
B. Regression Analysis	56
C. Results	60
D. Discussion of Results	61
1. Comparison of the Correlations	66
2. Effect of Equivalent Drop Diameter on Eccentricity	72
3. Effect of Physical Properties on Eccentricity	76
V. CONCLUSION	84
VI. RECOMMENDATIONS	88
VII. APPENDIX	90
A. Materials	91
B. Data Tables	92
C. Results	102
D. Nomenclature	110

	<u>Page</u>
VIII. BIBLIOGRAPHY	112
IX. ACKNOWLEDGEMENT	114
X. VITA	115

LIST OF FIGURES

FIGURE	<u>Page</u>
1. Flow pattern round a falling solid sphere .	7
2. Terminal velocities of liquid drops in liquid media as a function of drop diameter . . .	10
3. Hu and Kintner correlation for terminal correlation for terminal velocity of liquid drops	10
4. Drag coefficient of liquid drops in liquid media as a function of Reynolds number . .	18
5. Circulation within a liquid drop.	18
6. A spheroidal shaped liquid drop	18
7. E versus d_e plots of Keith and Hixson . . .	24
8. E versus d_e plots of Garner and Tayeban . .	24
9. E versus d_e plots of Klee and Treybal . . .	26
10. $\frac{\Delta E}{\Delta d_e}$ versus $\frac{\Delta \rho^{0.5}}{\sigma_i}$ plot of Klee and Treybal . .	26
11. Forces acting on surface of a drop	29
12. Eccentricity of fluid particles as a function of Eotvos number	29
13. Plot j_{ds} versus Re_s	37
14. Plot j_{dl} versus Re_l	37
15. Schematic diagram of the apparatus for studying the shape of liquid droplets . . .	44
16. Comparison of observed eccentricity with those calculated from correlation 1 for all data points	67

FIGURE	<u>Page</u>
17. Comparison of observed eccentricity with those calculated from correlation 2 for all data points (Harmathy's correlation).	68
18. Comparison of observed eccentricity with those calculated from correlation 3 for all data points	69
19. Comparison of observed eccentricity with those calculated from correlation 4 for all data points	70
20. Observed eccentricity and calculated eccentricity as a function of equivalent drop diameter "in the 0.31 to 0.72 c.p. μ_c region".	73
21. Observed eccentricity and calculated eccentricity as a function of equivalent drop diameter "in the 0.85 to 4.0 c.p. μ_c region".	74
22. Observed eccentricity and calculated eccentricity as a function of equivalent drop diameter "in the 4.7 to 45.9 c.p. μ_c region".	75
23. Keith and Hixson eccentricity data investigated in this work	95
24. Plot $\ln(E \cdot Re)$ versus $\ln(E \ddot{o} \cdot We)$	109

LIST OF TABLES

TABLE	<u>Page</u>
I. List of Liquid-Liquid Systems Experimentally Studied	41
II. Correlations 1 through 4 with 95 Percent Confidence Limits of Key Parameters	62
III. Range of Physical Properties of the Systems and Certain Important Dimensionless Groups Covered in this Study	64
IV. List of Liquid-Liquid Systems and Their Sources	92
V. Physical Properties, Equivalent Diameter, Velocity, and Eccentricity of Droplets	96
VI. Dimensionless Groups	99
VII. Observed Eccentricity and Calculated Eccentricities Calculated by Correlations 1 through 4	104

I. INTRODUCTION

Many of the physical separation and chemical reaction operations in the field of chemical engineering require intimate contact of two immiscible fluids. Examples of these operations are gas absorption and liquid-liquid extraction. In the case of liquid-liquid systems, often one liquid is dispersed in the form of droplets in the other liquid in order to provide a maximum surface contact area between the two liquids. A familiar example of one type of equipment used for this purpose is a spray column. The design of such equipment requires knowledge of droplet mechanics, interfacial area (shape and number of droplets), gross flow patterns of the two phases, and the rate of interphase mass transfer.

Liquid droplets traveling through a liquid medium behave differently than solid spherical particles. When a liquid drop moves through another liquid medium, the following may occur: (a) circulation of the constituent liquid may take place inside the drop, (b) the drop may be distorted in shape, (c) prolate-oblate oscillation in drop shape may occur, or (d) the droplet may breakup into smaller droplets (4). Droplets

in liquid media fall or rise, depending upon the densities of the two liquids. Small drops travel straight, but as the size increases, motion becomes zigzag depending upon the physical properties of the systems. The velocity of the drops in liquid media can be calculated from the empirical correlation of Hu and Kintner (8).

The surface area of a drop depends not only upon its size, but on its shape. Since liquid drops are seldom perfect spheres, their surface area can not be accurately calculated by a knowledge of volume alone. As the droplet becomes distorted, its surface area increases. Since heat and mass transfer rates depend on interfacial area of the dispersed phase, it is very important to know the accurate surface area of the drops. The rate of mass transfer to droplets is also related to the shape of the dispersed particle as indicated by the work of Skelland and Cornish (21). Therefore, the object of this investigation is to obtain an accurate method of predicting the surface area of distorted non-oscillating drops moving in liquid media from a knowledge of system physical properties and droplet volume.

II. LITERATURE REVIEW

A. Introduction to Drop Mechanics

Particle mechanics is of considerable importance in the field of chemical engineering. The following cases may occur in practice: (1) the motion of solid particles in a gas or liquid media, (2) the motion of gas bubbles in a liquid media, (3) the motion of liquid droplets in a gaseous media, and (4), the case with which the present work is concerned, motion of liquid droplets in a liquid medium.

The velocity and the drag coefficients of particles have been extensively studied for all the cases mentioned above, and a good summary is available in the Chemical Engineers Handbook (18). The gas and liquid particles differ from rigid particles in that their shape deforms easily and in that motion (circulation) occurs within the particle. Investigations of the shape of liquid droplets and their deformation are reported in the literature (6, 7, 11, 13). There is, to this date, no satisfactory empirical or theoretical method available which can be used to predict the shape of liquid droplets when in

motion relative to another liquid.

A brief survey of particle mechanics connected with the present investigation is presented here.

B. Mechanics of Rigid Particles

The mechanics of rigid particles is the simplest of those mentioned above, and an understanding of it is necessary before we extend the investigation to liquid droplets.

A rigid particle in motion, under the influence of a uniform gravitational field, accelerates first and finally reaches a constant maximum velocity known as the terminal velocity. The friction between the particle and fluid, arising from relative motion between the two, increases with velocity until the frictional resistance or drag equals the accelerating force and the terminal velocity results. A mathematical relation between the forces exerted on the particle during motion is presented in Brown (2). The drag force on the particle is given by (18)

$$F_d = \frac{C A_p \rho_c U}{2 \epsilon_c} \quad (2.1)$$

and the terminal velocity is given by,

$$U_t = \sqrt{\frac{2 g M (\rho_d - \rho_c)}{\rho_c \rho_d A_p C}} \quad (2.2)$$

where,

M = mass of particle, lb_m

F_d = drag force on the particle, lb force

C = drag coefficient

A_p = projected area of the particle in the
direction of motion, ft^2

U = velocity of particle, ft/sec

U_t = terminal velocity of particle, ft/sec

ρ_d = density of particle, lb_m/ft^3

ρ_c = density of liquid, lb_m/ft^3

The drag coefficient, C , is a function of the Reynolds number, $Re (=d_e U_t \rho_c \mu_c)$. For Reynolds numbers less than 0.3, flow is in the Stokes' Law realm, i.e., laminar flow region. Drag is fully viscous in this region, and the viscosity of the fluid is an important factor in determining the resistance to flow. Drag also depends upon the shape and orientation of the particle with respect to the direction of motion. In the Newton's

Law region, i.e., Re between 1,000 and 200,000, the particle assumes a position which offers maximum resistance (18).

Figure 1 represents the flow pattern round a falling solid sphere. Figure 1a represents flow lines where Stokes' Law holds ($Re < 1$). Figure 1b is for higher velocities. The boundary layer increases in thickness from point A around the sphere until at a certain point, S, separation occurs and a new streamline is formed on the sphere. At still higher sphere velocities, eddies and vortex rings are formed behind the sphere (Figure 1c). At further increasing speeds, the separation point of the streamlines moves forward along the sphere to point 'A'. The eddies introduce increased resistance to flow, and the viscosity of the continuous phase liquid becomes less important. The viscosity becomes a negligible factor in determining the resistance when the flow conditions become completely turbulent ($Re > 1,000$). The drag coefficient, C , is fairly constant ($C=0.44$) in the Re range 1,000 - 200,000.

C. Mechanics of Droplets in Liquid-Liquid Systems

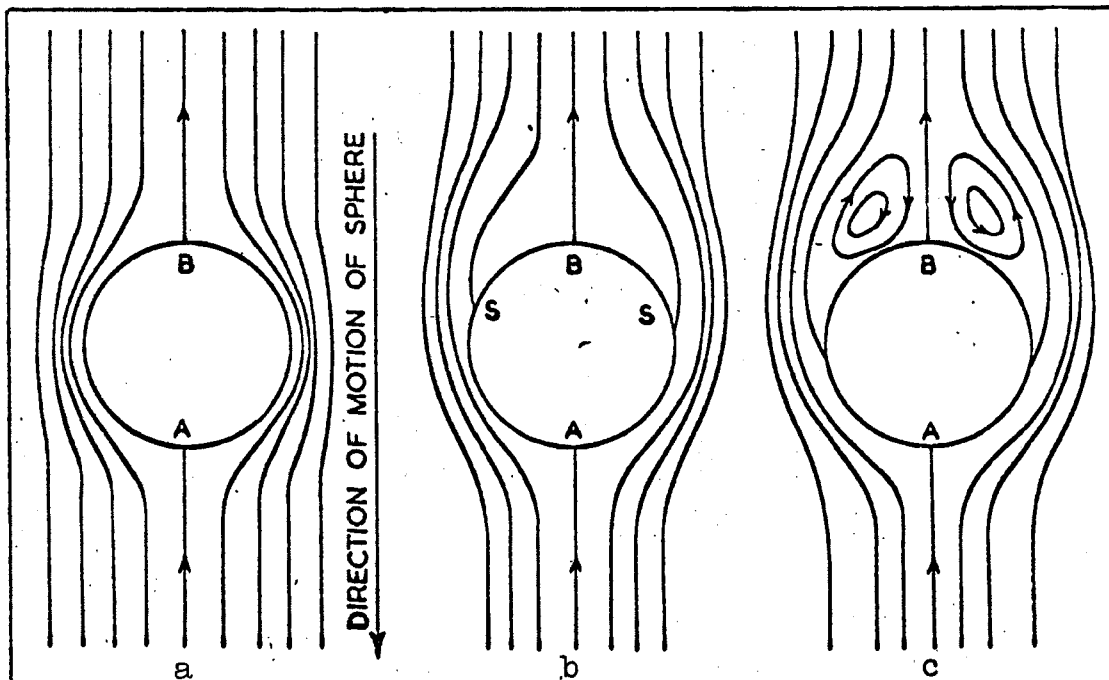


Figure 1. Flow pattern around a falling solid sphere.

1. Formation of Liquid Droplets. Drops are generally formed by forcing the liquid through a nozzle or nozzles into the continuous phase liquid. Pulsating sieve plates, rotating discs, and other means are also used to form the liquid droplets.

For drop formation from single nozzles at low nozzle flow rates, drops form individually at the nozzle tip and grow in size until bouyance force (or gravitational force) overcomes interfacial tension forces holding the droplet to the nozzle, and the drop is released. At higher flow rates, jets, are formed or in some cases even atomized sprays of droplets may result (11). The rate of drop formation affects the drop volume after detachment (10). Null and Johnson (16) give a correlation which predicts the volume of individual drops formed at single nozzles within 20 percent accuracy throughout the range of nozzle flow rates for which uniform drop sizes are obtained.

2. Terminal Velocity. In case of liquid-liquid systems, the droplet fall (or rise) velocity, shape, drag coefficient, and the internal circulation within the liquid droplets are all interdependent. The fluid

mechanics aspect of the problem is very complex and does not yield to an easy analytical solution.

Like solid particles, droplets after formation first accelerate and then reach a constant terminal velocity. The terminal velocity depends upon the size of the drop and physical properties of the system. Figure 2 is a typical plot of terminal velocity versus equivalent drop diameter. Curves similar to Figure 2 have been reported in literature by several authors (4, 8, 11, 13). The terminal velocity increases almost linearly with drop diameter up to a certain point, region 1 to 2 in the Figure 2. Thereafter, the slope decreases and a peak is reached (point 3). With further increases in drop diameter, the terminal velocity starts decreasing (region 3 to 4) and then gradually the curve becomes almost horizontal (region 4 to 5), i.e., the terminal velocity becomes practically constant. A stage is reached at which any further increase in drop diameter results in the breaking of the drop into smaller droplets. For comparison purposes, the dashed curve on Figure 2 represents the qualitative behavior of a solid sphere. Notice that no peak is observed in the region where liquid droplets exhibit a peak.

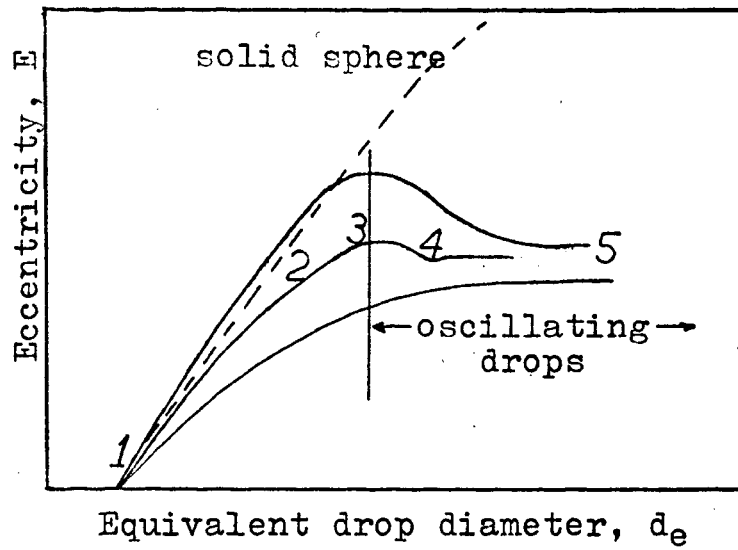


Figure 2. Terminal velocities of liquid drops in liquid media as a function of drop diameter.

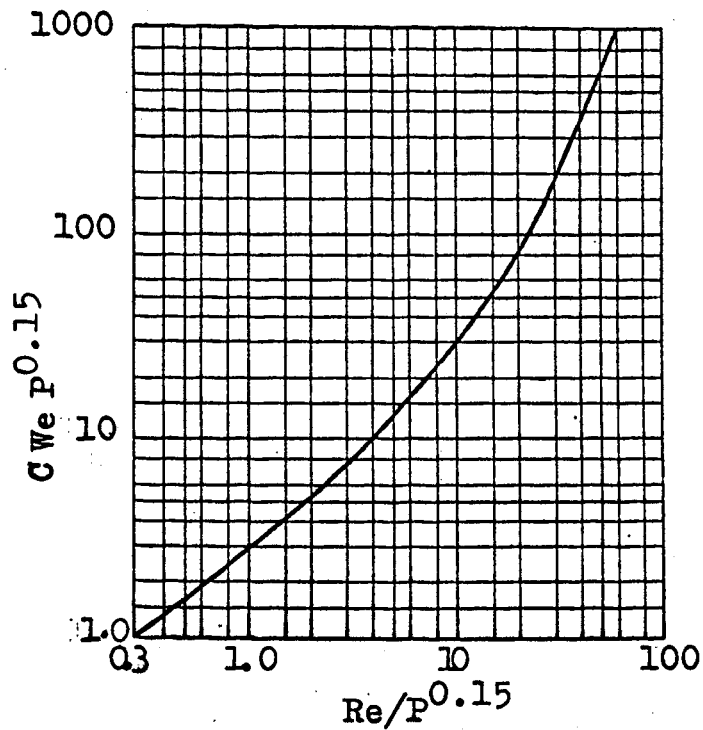


Figure 3. Hu and Kintner correlation for terminal velocity of liquid drops.(8).

The peak velocity is the maximum velocity that a drop in any liquid system can attain. Liquid systems with smaller density differences, $\Delta\rho$, between the continuous phase and dispersed phase liquids have lower peak velocities than those systems having greater $\Delta\rho$ (10,11). At the peak velocity, drops start oscillating between the oblate and prolate shape. Drops, larger in size than those corresponding to the peak velocity (point 3), have oscillations and occasionally move in a zigzag path instead of a straight path as smaller size drops. The actual vectorial velocity of drops having zigzag motion is higher than the apparent measured velocity (8). Calculation of the peak velocity is described in the following section.

Hu and Kintner (8) have presented a correlation for nine liquid systems in the form of a single curve, Figure 3 relates the drag coefficient ($C = \frac{4}{3} \frac{\Delta\rho d_e g}{\rho_c U_t^2}$), Weber number ($We = \frac{\rho_c d_e U_t^2}{\sigma_i}$), Reynolds number ($Re = \frac{d_e U_t \rho_c}{\mu_c}$), and a physical property group ($P = \frac{\rho_c^2 \sigma_i^3}{g \mu_c^4 \Delta\rho}$). The curve which is a plot of $\log(C \cdot We \cdot P^{0.15})$ versus $\log(Re \cdot P^{0.15})$, can be used directly to predict the terminal velocity of a drop when equivalent droplet diameter and physical properties of the system are known.

The error involved in the prediction of U_t is generally less than 10 percent. The range of Re covered in the investigation was 10 to 2,200.

Klee and Treybal (13) studied the fall of single liquid drops for eleven systems in which the interfacial tension ranged from 0.3 to 42.4 dynes/cm. Through dimensional analysis of

$$f(d_e, U_t, g, \mu_c, \mu_d, \rho_c, \Delta\rho, \sigma_i)^* = 0 \quad (2.3)$$

they obtained the relation

$$\left(\frac{\mu_c}{\mu_d}\right)^a \left(\frac{\Delta\rho}{\rho_c}\right)^b Re^e We^h C^j = m \quad (2.4)$$

The exponents 'a', 'b', 'e', 'h', and 'j'; and coefficient 'm' are empirical constants. They proposed two equations for calculating the terminal velocity of the drops:

$$Re = 22.2 C^{-5.18} We^{-0.169} \quad (2.5)$$

$$Re = 0.00418 C^{2.91} We^{-1.81} \quad (2.6)$$

Equation (2.5) applies to the region where U_t increases with drop diameter, and equation (2.6) applies to the terminal velocity region to the right of the peak (Figure 2). The errors involved in the use of equation (2.5) and equation (2.6) for the authors' (Klee and Treybal) data are correspondingly 4.15 and 2.82 percent. The

* Symbols are defined in Nomenclature, page 110.

data of Hu and Kintner (8) show 15.2 and 5.5 percent error respectively, for the equations (2.5) and (2.6). Klee and Treybal inferred that the Hu and Kintner correlation is good for high interfacial tension systems, and thus equations (2.5) and (2.6) are good for systems having low interfacial tension. The velocity data of Keith and Hixson (11) show a 4.5 percent error when compared with the Klee and Treybal correlations.

Johnson and Braida (10) report verification of the Hu and Kintner correlation with their data of organic-aqueous systems. However, they suggest a continuous phase viscosity correction factor for the correlation to correct for the effect of high continuous phase viscosities. Their new correlation is a plot of $\ln \left[C \cdot We \cdot P^{0.15} / (\mu_c / \mu_d)^{0.14} \right]$ versus $\ln(Re/P^{0.15})$. This new correlation fits all their data, including systems which had 28.5, 60, and 75 percent glycerine as the continuous phase and which could not be fitted on the Hu and Kintner plot.

In the turbulent region ($Re > 500$), Harmathy (7) shows that the terminal velocity is independent of drop diameter.

$$U_t = 1.53 \left(\frac{g \Delta \rho \sigma}{\rho_c} \right)^{\frac{1}{2}} \quad (2.7)$$

Elzinga and Banchero (4) studied the effect of surface active agents on the water and Dowtherm A+E system. Comparison of the observed terminal velocity with those calculated from the Klee and Treybal (13) and Hu and Kintner (8) correlations show that very pure liquids have higher velocities than those predicted by both of the correlations. The correlation of Klee and Treybal predict terminal velocities which are close to the observed value for the systems treated with surfactant powder. Elzinga and Banchero conclude that surfactants affect drop velocities regardless of changes in such physical properties of the systems as interfacial tension, density, and viscosity.

3. Peak Velocity. The peak velocity has been described in the previous section. The distinct break in the Hu and Kintner correlation, Figure 3, is in the Reynolds number region approximately corresponding to that where the peak terminal velocity occurs. Hu and Kintner found that at the peak velocity

$$(U_t)_p = 1.23 \left(\frac{\sigma_i}{\mu_c} \right) P^{-0.238} \quad (2.8)$$

$$\text{or} \quad (U_t)_p = 1.23 \left(\frac{\sigma_i}{\mu_c} \right) \left(\frac{\rho_c^2 \sigma_i^3}{8\mu_c^4 \Delta\rho} \right)^{-0.238} \quad (2.9)$$

and peak velocity, $(U_t)_p$, is independent of drop diameter. They further observed that

$$(We)_p = 3.58 \quad (2.10)$$

and thus

$$(d_e)_p = 3.58 \left(\frac{\sigma_i}{\rho_c} \right) / (U_t)_p^2 \quad (2.11)$$

Johnson and Braida (10) noticed that the drop begins to oscillate as the drop size approaches the peak value of the terminal velocity. The equivalent drop diameter at peak terminal velocity, $(d_e)_p$, can also be obtained by simultaneously solving Klee and Treybal's equations (Equation 2.5 and 2.6) given on page 12.

4. Wall Effect on Velocity. When the annular space between drop and walls holding continuous media is small, wall effects appear. The terminal velocity of the drop is reduced, and in some cases, the shape of the droplet may be altered because of the proximity of the walls. The following relation of Strom and Kintner (19) gives an estimate of the reduction of droplet velocity as a function of the droplet to column diameter ratio:

$$U_t = U_\infty \left[1 - (d_e/D)^2 \right]^{1.43} \quad d_e/D < 0.5 \quad (2.12)$$

where, d_e = equivalent drop diameter, cm

D = diameter of the column, cm

U_t = terminal velocity in restricted media, cm/sec

U_∞ = terminal velocity of drop in infinite media, cm/sec

The proximity of the wall causes turbulence in the continuous phase and induces oscillations in the drop shape.

Harmathy (7) presents the correlation

$$\frac{U_t}{U_\infty} = \frac{0.88}{(Eö)^{\frac{1}{4}}} \frac{1 - \left(\frac{d_e}{D}\right)^2}{\sqrt{1 + \left(\frac{d_e}{D}\right)^4}} \left[1 - \frac{2}{3} \frac{Eö}{1 + Eö} \left(\frac{d_e}{D}\right)^{3/2} \right] \quad 0 \leq \frac{d_e}{D} \leq 1.3 \quad (2.13)$$

which can be used to predict the terminal velocity of drops, including cylindrical drops, in the region $Re > 500$.

5. Drag Coefficient. The force balance (9) for the vertical motion of a drop through a stagnant continuous phase of infinite extent can be written as:

$$\frac{\pi}{6} d_e^3 \rho_d \frac{dU}{dt} = \frac{\pi}{6} d_e^3 g (\rho_d - \rho_c) - \frac{\pi}{4} C d_e^2 \frac{\rho_c U^2}{2} \quad (2.14)$$

The drag coefficient, C , is defined as:

$$C = \frac{\text{drag}}{\text{frontal area}} \times 1/(\rho_c U_t^2 / 2g_c) \quad (2.15)$$

Because of the undefined shape of a liquid drop, the geometry is usually assumed to be spherical and the value of C allowed to vary to adjust this assumption to the actual facts. To integrate equation (2.14), the drag coefficient must be known as a function of other variables.

Figure 4 is a typical plot of C against Re on a log log scale. Hu and Kintner's studies (8) of the drag coefficient of liquid drops for nine systems show no marked difference between the C of liquid drops and that of rigid spheres up to a $Re=300$. After the limiting Re range is passed, the $\ln(C)$ versus $\ln(Re)$ curves for the liquid systems depart from the curve for solid spheres, but still retain a somewhat similar pattern. At first, C decreases only very slightly with increasing Re for a rather large Re range, but when the Re reaches a certain value, C starts to increase abruptly within a narrow range. The onset of drop oscillation is the cause of this abrupt change. After the abrupt rise, the curve proceeds at a more or less constant slope until the critical drop size is reached and droplet breakup occurs. The range of Reynolds number where the drag coefficient stays somewhat constant corresponds to the region where zigzag motion and drop oscillation occur. The probable reason that C remains constant is that the apparent velocity is lower than the actual vectorial velocity.

Drag coefficient, C , versus Reynolds number, Re , curves similar to those of Hu and Kintner were obtained by Licht and Narasimhamurty (15), and also by Klee and

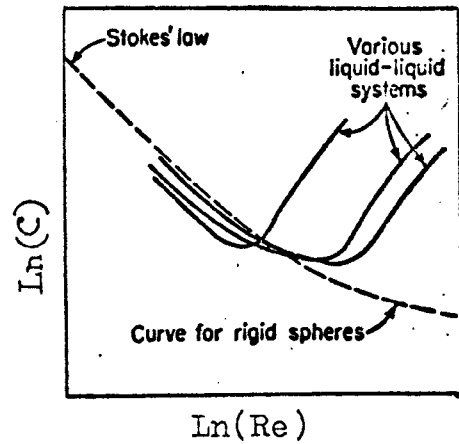


Figure 4. Drag coefficient of liquid drops in liquid media as a function of Reynold number. (23).

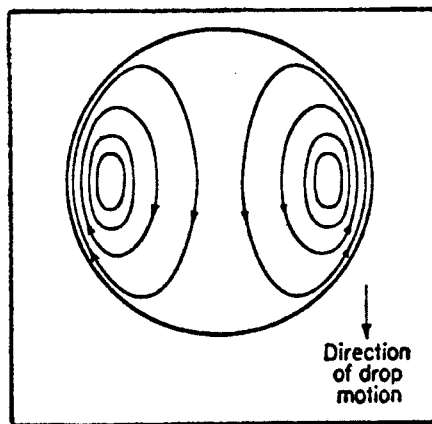


Figure 5. Circulation within a liquid drop. (23).

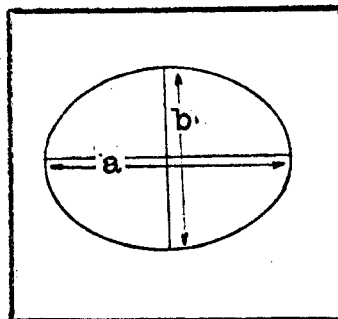


Figure 6. A spheroidal shaped liquid drop.

Treybal (13). The drag coefficient for all ten systems that Klee and Treybal studied fell below the curve for rigid spheres in the low Re region. This difference in behavior is very likely because of internal circulation within the drops. Johnson and Braida (10) found that C versus Re curves for liquid drops in the low Re range fall close to that for solid spheres. They observed that the slight difference between the curves for solid spheres and liquid drops is due to possible distortion of the shape of liquid drops.

Harmathy (7) by dimensional analysis has shown that

$$C = f(E\ddot{o}) \quad (2.16)$$

His plots of C^*/C_s against $E\ddot{o}$ resulted in a smooth curve and support his theory. C^* is the drag coefficient of the drop and C_s is the drag coefficient of a sphere having a diameter equivalent to that of the drop, $E\ddot{o}$ is Eötvös number.

Elzinga and Banchemo (4) report C versus Re curves in the low Re region for liquid droplets. The curves show the same general pattern as found by previous authors and fall below the curve for solid spheres. The previous workers explained the lower values of C for liquid drops by attributing the phenomena totally to the absence of

skin friction because of circulation within the droplets. Elzinga and Banchero point out that skin friction is a small fraction, only about ten percent of the total drag in the low Reynolds number region. The observed reduction in C for liquid drops is sometimes as high as forty percent. Therefore, internal circulation must have additional effects on drag besides lowering the skin friction.

6. Circulation within Droplets (25). When liquid droplets travel through a viscous continuous phase, the surface of the drops is carried from the forward stagnation point to the rear by shear at the interface. Unlike a rigid sphere, the droplet surface is mobile. It has been observed that the lower the interfacial tension, the higher the mobility of the drop surface; therefore, the possibility of internal circulation is increased. The mobility of the drop surface and internal circulation decrease the drop drag coefficient below that for solid spheres. The effect of internal circulation is to reduce the boundary layer thickness and, for the extreme case, i.e., full internal circulation, the boundary layer thickness is zero. The critical drop diameter at which full internal circulation is reached is given by Bond and Newton (1) in the following empirical expression:

$$(d_e)_c = 3.0 \frac{\varepsilon_c \sigma_i}{\varepsilon |\rho_d - \rho_c|} \quad (2.17)$$

where, $(d_e)_c$ is critical drop diameter.

Bond and Newton's data show that the circulation begins where drop diameter, d_e , is about $0.1(d_e)_c$, and is completed when $d_e = (d_e)_c$. Thus, the above empirical equation must be considered as only an approximation.

Surface-active substances, which are strongly absorbed at liquid-liquid interfaces, may prevent surface motion and internal circulation by making the surface relatively rigid. It can be expected that rates of fall (or rise) will be closer to those expected for rigid spheres. This has been widely observed (4).

7. Shape. A moving drop is distorted by the local forces acting on its surface. These forces are caused by differences in hydrostatic head, shear stress, internal and external fluid motion, and interfacial tension. The distortions are of two basic types: those of an equilibrium nature, and those of an oscillating nature resulting from vibrations about this equilibrium position (9).

The drag coefficient is a function of the shape of the moving particle. Any distortion in the shape will have a marked effect on the motion of the fluid particle. In addition, such distortion would have an effect on the magnitude of the surface area of the drop and, thus, on the rate of heat and mass transfer.

The shape of fluid particles is determined by the forces acting along their surface. The pressure exerted by the surrounding fluid on a moving sphere is not uniform. The pressure distribution is not exactly known even for the simple geometry of a sphere. Within a drop, since the fluid motion is slight, the pressure is essentially uniform except for gravitational head. Since the pressure distribution around moving liquid droplets is not known, the theoretical calculation of the shape can be assumed to be spheroidal (see Figure 6) with axis in the direction of motion and deformation expressed as eccentricity.

$$\text{Eccentricity, } E = \frac{a}{b}$$

where, a = horizontal diameter

and b = vertical diameter

Qualitative observations of droplet shape by Licht and Narasimhamurty (15) in 1955 are summarized below:

1. The smaller size drops are less deformed than

- larger ones and are more nearly spherical.
2. Some of the deformed drops in the larger size show unsteady-state vibrations (oscillations) in shape.
 3. Deformed but non-oscillating droplets fall with an uniform velocity.
 4. Drops with vibrations show unequal velocities of fall when the time interval for the measurements of droplet velocity is reduced.
 5. Larger drops fall in zigzag paths.
 6. In many cases there is no axial symmetry in the shape of the drops.

Keith and Hixson (11) photographed moving drops and measured the ratio of maximum to minimum diameter. The eccentricity which they reported is the average of a large number of drops (of the same volume) which were sometimes oscillating. They observed that eccentricity of drops is directly proportional to drop size and difference in liquid densities and inversely proportional to interfacial tension. The eccentricity varies almost linearly with equivalent diameter. (See Figure 7.)

Klee and Treybal (13) also reported observations similar to the above. They measured the average

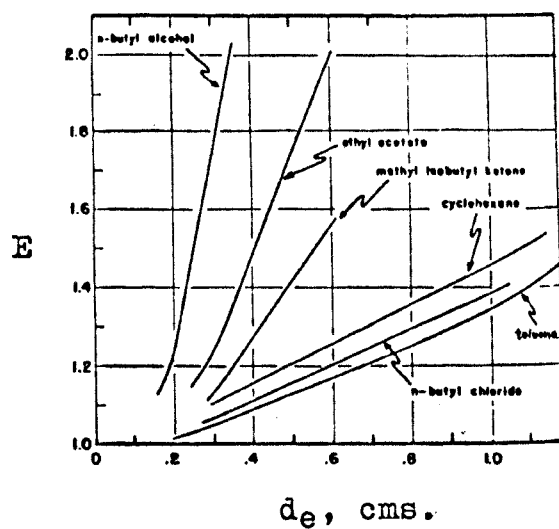


Figure 7. E versus d_e plots of Keith and Hixson (11).

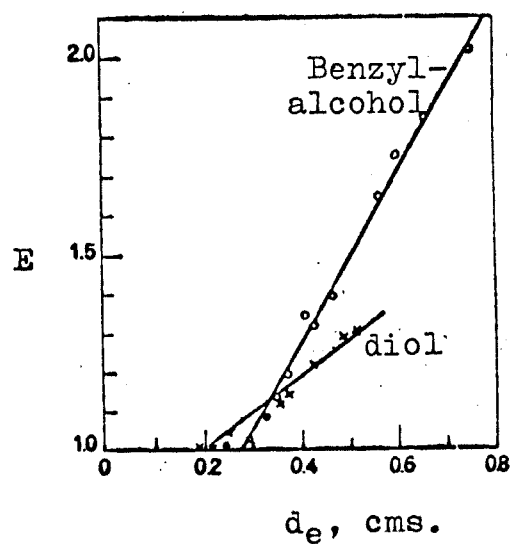


Figure 8. E versus d_e plots of Garner and Tayeban (6).

eccentricity of the drops and found that the relation between the eccentricity and equivalent drop diameter is substantially linear for all but the smallest drop sizes. (See Figure 9.) They found that the logarithm of the slope of the slope of eccentricity curves of the different systems, i.e., $\log\left(\frac{\Delta E}{\Delta d_e}\right)$ of the systems, when plotted against $\log\left(\frac{\Delta \rho^{0.5}}{\sigma_i}\right)$ of the systems resulted in a straight line. (See Figure 10.)

Neither Keith and Hixson nor Klee and Treybal have presented any correlation which could be used to predict the eccentricity of liquid drops of a system. The E versus d_e graphs are good only for those systems for which they are plotted.

Although, the slope of E versus d_e curves of a system for which $\Delta \rho$ and σ_i are known can be calculated from Klee and Treybal's graphical correlation of $\log\left(\frac{\Delta E}{\Delta d_e}\right)$ versus $\log\left(\frac{\Delta \rho^{0.5}}{\sigma_i}\right)$, the slope is not useful unless at least one value of E corresponding to d_e is known. Notice that the curves do not pass through the origin. (See Figures 7, 8 and 9.) Therefore, the point at the origin can not be used with their correlation. Even if one value of the eccentricity and corresponding equivalent drop diameter were known, this method has a

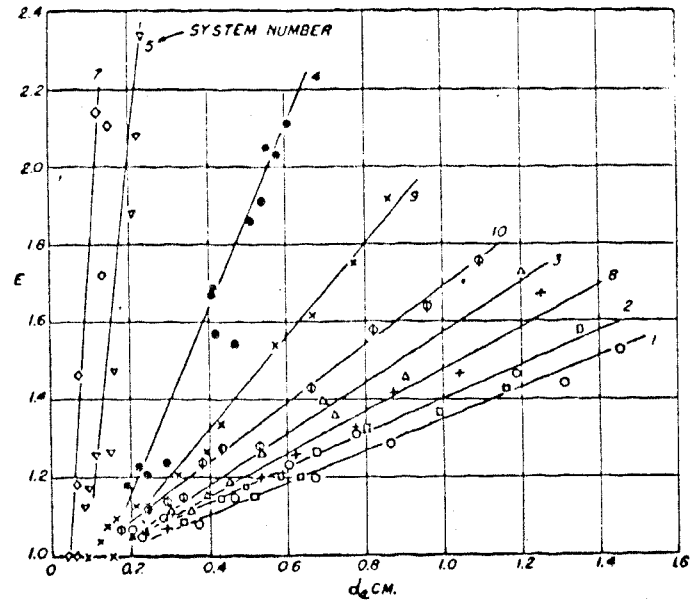


Figure 9. E versus d_e plots of Klee and Treybal (13).

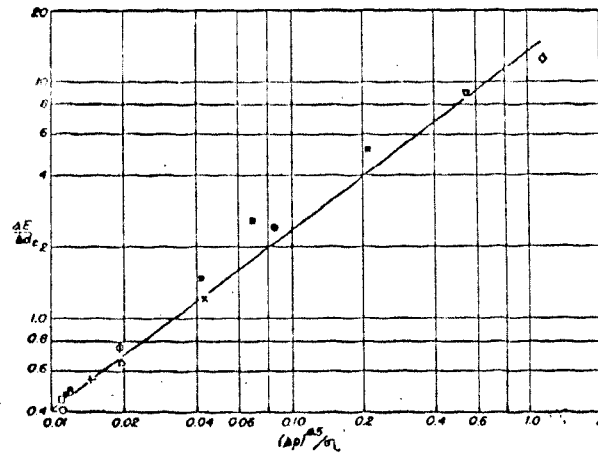


Figure 10. $\frac{\Delta E}{\Delta d_e}$ versus $\left(\frac{\Delta \rho}{\sigma_1}\right)^5$ plot of Klee and Treybal (13).

serious drawback in that the calculated eccentricity may not be accurate enough for small size droplets for which eccentricity, E , is not directly linear with d_e .

It has been observed that viscosity of the dispersed phase liquid affects the magnitude of the drop deformation. Garner and Tayeban (6) noticed, Figure 8, that 2-ethylhexane 1.3 diol drops ($\mu_d = 85$ c.p.) have lower eccentricities than corresponding benzyl alcohol drops ($\mu_d = 5.3$ c.p.) although the density differences and interfacial tensions of the two systems are very close. The continuous phase liquid was water in both the cases.

Elzinga and Banchemo (4) have reported that the addition of minute quantities of a surface-active agent greatly reduced droplet distortion for one of their systems. They speculate that the surface-active agent may have reduced internal circulation and that the reduced internal circulation resulted in less deformation. They pointed out that easily measured properties such as interfacial tension, density, and viscosity would not detect the presence of surface-active agents.

Harmathy (7) suggests that the shape of drops is a function of Eötvös number ($= \frac{g \Delta \rho d_e^2}{\sigma_i}$). An analytical study of the forces acting on the moving drop which leads to this conclusion is given below.

The following assumptions are made to simplify the analysis:

1. The drop is moving upward at its terminal velocity, i.e., the accelerating forces are balanced by the retarding forces.
2. The drop is symmetrical about its vertical axis, and its meridian curve is $r = f(z)$ (Figure 11).

The equilibrium of the forces is expressed by

$$p_i = p_{hd} + p_r + p_{hs} \quad (2.18)$$

where,
$$p_i = p_{i0} + \rho_d g z \quad (2.19)$$

$$p_{hs} = p_a + \rho_c g z + \rho_c g h \quad (2.20)$$

$$p_r = \sigma \left(\frac{1}{R_1} + \frac{1}{R_2} \right) \quad (2.21)$$

and under turbulent flow conditions

$$p_{hd} = \frac{\rho_c u_t^2}{2} \bar{p}_{hd} \quad (\text{shape}, \alpha) \quad (2.22)$$

for $z = 0$, $R_1 = R_2 = R_0$, and $\bar{p}_{hd} = 1$

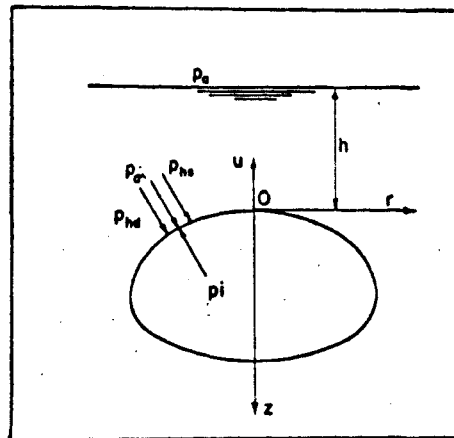


Figure 11. Forces acting on surface of a drop (7).

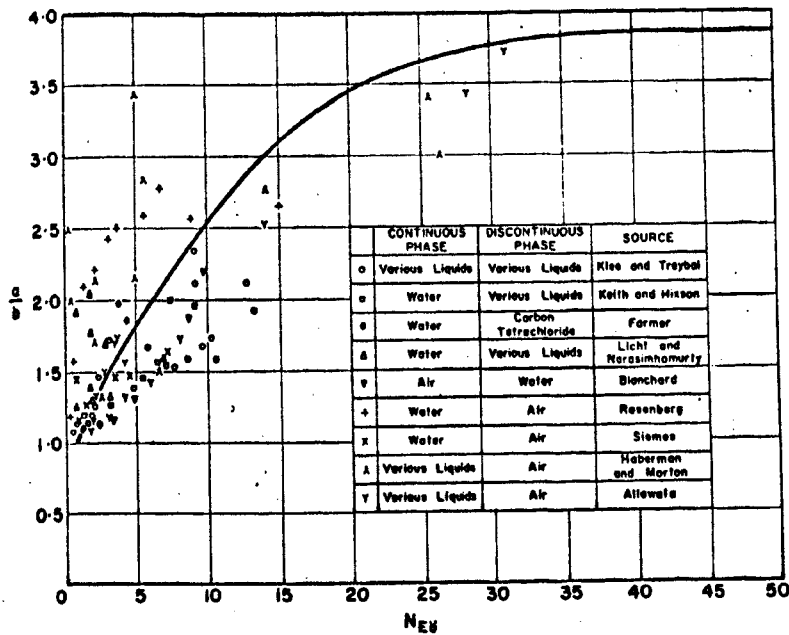


Figure 12. Eccentricity of fluid particles as a function of Eötvös number (7).

$$\text{thus } p_{i0} = p_a + \rho_c g h + \rho_c g z + \sigma \left(\frac{1}{R_0} + \frac{1}{R_1} \right) + \frac{\rho_c U_t^2}{2} \quad (2.23)$$

combining equations (2.18) and (2.23) one has

$$(\rho_c - \rho_d) g z + \sigma \left(\frac{1}{R_1} + \frac{1}{R_2} + \frac{1}{R_0} \right) - \frac{\rho_c U_t^2}{2} \left[1 - \bar{p}_{hd}(\text{shape}, \alpha) \right] = 0 \quad (2.24)$$

using 'de' as the characteristic length equation (2.24) in dimensionless form becomes

$$\frac{g \Delta \rho_d d_e^2}{\sigma_i} \bar{z} + \frac{1}{\bar{R}_1} + \frac{1}{\bar{R}_2} - \frac{2}{\bar{R}_0} - \frac{1}{2} \frac{\rho_c d_e U_t^2}{\sigma_i} \left[1 - \bar{p}_{hd}(\text{shape}, \alpha) \right] = 0 \quad (2.25)$$

where, $\bar{z} = z/d_e$, $\bar{R}_0 = R_0/d_e$, $\bar{R}_1 = R_1/d_e$, and $\bar{R}_2 = R_2/d_e$

Equation (2.25) represents the relationship between the shape of the drop and the characteristics of the drop.

It can be assumed to represent a relationship of the form

$$f_1(\text{shape}, \frac{g \Delta \rho_d d_e^2}{\sigma_i}, \frac{\rho_c d_e U_t^2}{\sigma_i}) = 0 \quad (2.26)$$

$$\text{or } f_1(\text{shape}, E\ddot{o}, We) = 0$$

In the turbulent flow region

$$U_t = \sqrt{\frac{4}{3C}} \sqrt{\frac{g \Delta \rho_d d_e}{\rho_c}} \quad (2.27)$$

$$\frac{\rho_c d_e U_t^2}{\sigma_i} = \frac{4}{3C} \frac{\rho_c d_e}{\sigma_i} \left(\frac{g \Delta \rho_d d_e}{\rho_c} \right) \quad (2.28)$$

$$We = \frac{4}{3C} E\ddot{o} \quad (2.29)$$

C is known to remain constant in turbulent flow region

(for solid particles, $1,000 < Re < 200,000$) and is a function of shape only. Therefore, from equation (2.29)

$$We = f_2(\text{shape}, Eö) \quad (2.30)$$

The Weber number, We , can be eliminated from equations (2.26) and (2.30) to give:

$$\text{Shape} = f_3(Eö) \quad (2.31)$$

This would indicate that in the turbulent flow region for a given particle shape and Eötvös number, the Weber group does not impose an additional restriction on equation (2.26). Although Harmathy chose to eliminate the Weber group, the following relation would have applied equally well in the turbulent region:

$$\text{Shape} = f_4(We) \quad (2.32)$$

Nomenclature of Harmathy:

p_i = internal pressure

p_{hd} = hydrodynamic pressure

p_{hs} = hydrostatic pressure

p_s = pressure due to interfacial forces

p_{i0} = internal pressure at the leading point '0'

p_a = atmospheric pressure

d_e = equivalent diameter of drop

- r = distance variable in the horizontal direction
 h, z = distance variable in the vertical direction
 α = latitude on the particle surface, dimensionless
 U_t = terminal velocity of the drop
 R_0 = principal curvature at point '0'
 R_1, R_2 = principal curvatures of drop surface
 C = $\frac{4}{3} \frac{\Delta \rho g d_e}{\rho_c U_t^2}$, drag coefficient
 $Eö$ = $\frac{\Delta \rho g d_e^2}{\sigma_i}$, Eötvös number
 We = $\frac{\rho_c d_e U_t^2}{\sigma_i}$, Weber number

Figure 12 is the plot of eccentricity against Eötvös number as obtained by Harmathy. Points show a large deviation from the smooth curve drawn by the author. Thus, Figure 12 does not exactly prove Harmathy's suggestion that shape or eccentricity of a drop is a function of the Eötvös number. However, Harmathy explains the scatter by assuming that some of the drops were oscillating and the reported eccentricity may not be the true average eccentricity. One should also remember that if equation (2.27) is not applicable (i.e., $Re < 1,000$) then one is restricted to the more general function

$$\text{Shape} = f(\text{We}, Eö)$$

Harmathy has not given any equation for the smooth curve in Figure 12. (However, the author of this thesis fitted a third order polynomial to the curve to aid in comparing the Harmathy correlation with those developed in this work.) Figure 12 includes some points which represent the eccentricity of liquid drops falling in air or of gas bubbles rising in liquid media. The curve, therefore, is not drawn strictly for the liquid-liquid systems alone, and this makes its use uncertain for predicting the eccentricity of liquid drops moving in liquid media.

It can be concluded, therefore, that there is no satisfactory method available which can be used to predict the eccentricity of liquid drops moving in liquid media.

8. Oscillation. In a certain characteristic range of diameters, liquid drops oscillate about their equilibrium shape. This phenomenon has been observed by many investigators (4,6,10,11,13,15,19). A table is given in Journal of Chemical and Engineering Data (14) which shows the equivalent droplet diameter ranges, obtained by visual observations, for a number of liquid-liquid systems where oscillation occurs. The presence of droplet oscillation is found to enhance the mass transfer and

heat transfer rates over those of non-oscillating drops (6).

According to the recent paper of Schroeder and Kintner (20) on drop oscillation:

1. Oscillation begins at or near the drop size corresponding to the peak velocity on the terminal velocity versus equivalent droplet diameter curve. (See Figure 2)
2. A necessary condition for oscillation is the presence of a vortex trail which is the driving mechanism for oscillation. This requires a Reynolds number of at least 200.
3. The oscillation described by the authors was not nozzle induced and did not decay with time.
4. Drop breakup is not caused by normal oscillation.
5. Velocity of fall does not affect the frequency of oscillation provided the vortex trail is present to drive the drop oscillation.
6. Dispersed phase viscosity has very little effect on oscillation except at high viscosities where it damps them out.
7. Continuous phase viscosity does not affect oscillation as long as the vortex trail is present. The vortex trail is damped out, however,

at a fairly low continuous phase viscosity.

8. The only type of oscillation the authors observed is the oblate-prolate type. This degenerates as the drops become large to random wobbling. Surface fluttering is observed in some systems but is not normally called oscillations.

9. Maximum Drop Size. Hu and Kintner (8) while investigating the fall of single liquid drops through water found that the maximum or critical drop size of the system, above which the droplet breaks into smaller droplets, is dependent on the criterion:

$$C \cdot We = \text{constant}$$

This leads to an equation for estimating the critical drop size from the density difference and interfacial tension of a system. The expression is

$$d_e = (1.452 \times 10^{-2} \frac{\sigma^i}{\Delta \rho})^{0.5} \quad (2.33)$$

10. Effect of Shape on Mass Transfer: Mass transfer coefficient are usually represented in form of a dimensionless relation, e.g.,

$$Sh = a_1 Re^{a_2} Sc^{a_3} \quad (2.34)$$

$$\frac{k_c d_1}{D_v} = a_1 \left(\frac{d_1 U \rho_c}{\mu_c} \right)^{a_2} \left(\frac{\mu_c}{\rho_c D_v} \right)^{a_3} \quad (2.35)$$

The dimensionless groups require the characteristic dimension d_1 representing the geometry of the body. In case of mass transfer between a spherical particle and the surrounding medium, Skelland and Cornish (21) have shown that the equivalent spherical diameter d_e is not the characteristic length but d_1 defined as

$$d_1 = \frac{\text{total surface area of the body}}{\text{perimeter of the body normal to flow}}$$

Skelland and Cornish (21) measured the individual continuous phase mass transfer coefficient, k_c , for oblate naphthalene spheroids in air. In their study they used spheroids of eccentricities 1, 5/4, 5/3, 2/1, 5/2, and 3/1, each having a major axis length of one inch. Their attempts to correlate k_c in the form

$$j_d = \frac{Sh}{Re \cdot Sc^{1/3}} = a_1 Re^{a_2} \quad (2.36)$$

are shown in the Figure 13 and 14. In Figure 13, characteristic dimension d_e was used, which resulted in a regular scattering of the data for the various spheroids. When the characteristic dimension d_1 was used all data fell on a smooth curve, Figure 14. The equation representing the curve in Figure 14 is

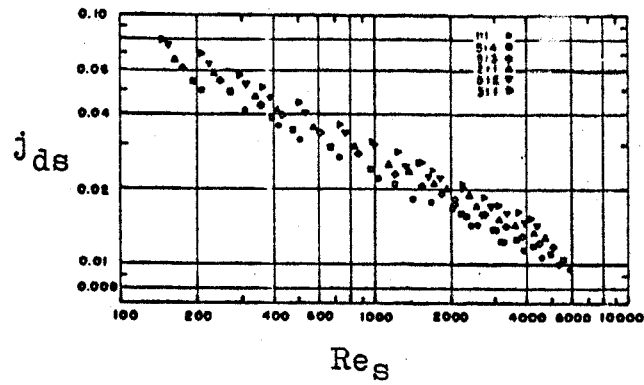


Figure 13. Plot j_{ds} versus Re_s (2).

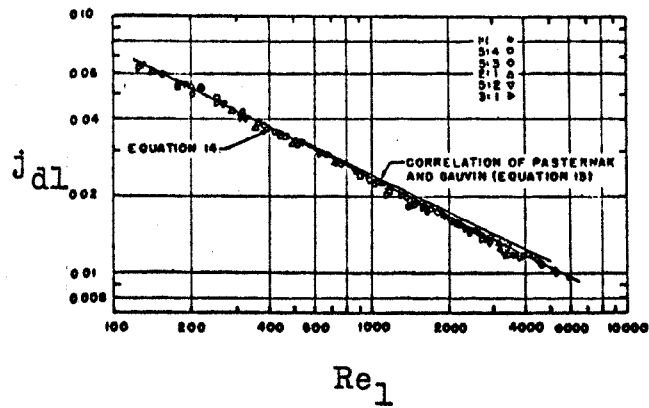
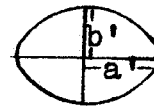


Figure 14. Plot j_{d1} versus Re_1 (2).

$$j_{d1} = 0.74 \operatorname{Re}_1^{-0.5} \quad (2.37)$$

The characteristic dimension, d_1 , in case of spheroids can be calculated theoretically, as shown below, if the equivalent diameter d_e and eccentricity E are known.

$$\text{Eccentricity } E = \frac{2a'}{2b'}$$



Volume of a spheroid formed by revolving the

$$\text{ellipse around its minor axis} = \frac{4}{3} \pi a'^2 b'$$

$$= \frac{4}{3} \pi E^2 b'^3$$

$$= \frac{\pi}{6} d_e^3$$

$$\text{Surface of spheroid} = 2\pi a'^2 + \frac{\pi b'^2}{e} \ln\left(\frac{1+e}{1-e}\right)$$

$$\text{Perimeter of spheroid at its major axis} = 2\pi a'$$

$$\frac{\text{Surface}}{\text{Perimeter}} = \frac{1}{2\pi a'} \left[2\pi a'^2 + \frac{\pi b'^2}{e} \ln\left(\frac{1+e}{1-e}\right) \right] \quad (2.38)$$

$$d_1 = \frac{1}{2} \left[2a' + \frac{b'^2}{a'} \frac{1}{e} \ln\left(\frac{1+e}{1-e}\right) \right]$$

$$= \frac{1}{2} \left[2b'E + \frac{b'^2}{Eb'} \frac{1}{e} \ln\left(\frac{1+e}{1-e}\right) \right]$$

$$= \frac{1}{E} b' \left[2E + \frac{1}{eE} \ln\left(\frac{1+e}{1-e}\right) \right]$$

$$\begin{aligned}
d_1 &= \frac{1}{2} \left(\frac{\pi d e^3}{6} \cdot \frac{3}{4\pi} \cdot \frac{1}{E^2} \right)^{1/3} \left[2E + \frac{1}{eE} \operatorname{Ln} \left(\frac{1+e}{1-e} \right) \right] \\
&= \frac{1}{2} \left(\frac{1}{8} \cdot \frac{d^3}{E^2} \right)^{1/3} \left[2E + \frac{1}{eE} \operatorname{Ln} \left(\frac{1+e}{1-e} \right) \right] \\
&= \frac{d e}{4} E^{2/3} \left[2E + \frac{1}{eE} \operatorname{Ln} \left(\frac{1+e}{1-e} \right) \right] \quad (2.39)
\end{aligned}$$

where, $e = \sqrt{1 - \left(\frac{1}{E}\right)^2}$.

III. EXPERIMENTAL

A. Object of Investigation

The object of this investigation is to obtain data on the deformation (eccentricity) of liquid drops falling in continuous liquid media. Special emphasis is placed on the eccentricity data of drops in the low viscosity media ($\mu_c < 0.7$ c.p.) and the high viscosity media ($\mu_c > 2.0$ c.p.). Besides eccentricity of the drops, their velocity and volume are also required. Densities, viscosities, and interfacial tension of the systems must also be determined.

B. Materials

All the chemicals used in this investigation are described in the appendix A.

C. Systems

The dispersed phase liquid together with the continuous phase liquid constitute a system. In all, thirteen systems were experimentally studied in this work, and are listed in Table I.

TABLE I

List of Liquid-Liquid Systems Experimentally Studied

No.	Dispersed Phase	Continuous Phase
1.	Nitrobenzene	Water
2.	Carbon tetrachloride	Water
3.	Water	Methyl isobutyl ketone
4.	Water	Hexane
5.	Bromobenzene	Water
6.	Aniline	Water
7.	Nitrobenzene	Glycol
8.	Water	Corn oil
9.	Glycol	Benzene
10.	Glycol	Hexane
11.	Water	Benzene
12.	Benzyl alcohol	Hexane
13.	Glycol	Methyl isobutyl ketone

Continuous and dispersed phase liquids were selected which were practically immiscible. Before starting any experiment the continuous and dispersed phase liquids were mutually saturated for 48 hours or more. This precaution was taken to avoid a change in volume of the drops because of mass transfer between the two phases. The exception was corn oil and water; this system was investigated without prior saturation. In all cases the continuous phase liquid had a density lower than that of dispersed phase liquid, and hence the droplets fell through the continuous phase.

D. Physical Properties

The relevant physical properties of interest in this work are densities and viscosities of the continuous and dispersed phases and the interfacial tension between the two phases.

All the physical properties were measured at the same temperature at which the eccentricity experiments were performed.

Density. Density measurements were made with a

pycnometer which was calibrated with distilled water. The density of distilled water was obtained from Chemical Engineers Handbook, 4th Edition (17).

Viscosity. Viscosity measurements were made with an Ostwald viscometer. The value of the viscosity of distilled water which was used for calibration was obtained from Handbook of Chemistry and Physics (26).

Interfacial Tension. The interfacial tension between the various continuous and dispersed phases was measured by means of a Cenco duNouy Ring Tensiometer (70540), series no. 630. The correction to the apparent interfacial tension was applied in accordance with the instructions of Central Scientific Company, Chicago, Illinois.

All the physical properties are listed in appendix B, Table IV.

E. Apparatus

A schematic diagram of the apparatus is shown in Figure 15. The major equipment used in this investigation

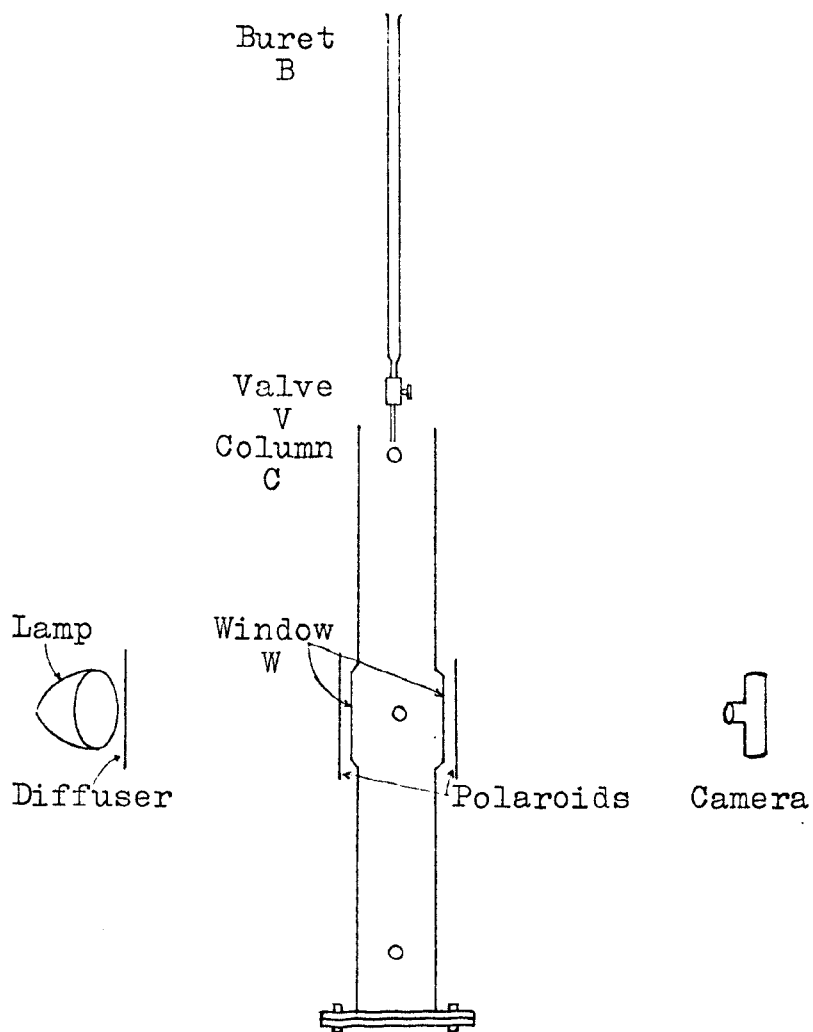


Figure 15. Schematic diagram of the apparatus for studying the shape of liquid droplets

is described below:

Glass Column. 'C', in Figure 15, is the Kimax glass column,

I.D. = 7.6 cm

Height= 93 cm

'W' and 'W' are two optically plane parallel glass windows in the middle of the column. The bottom of the column is blank flanged with a stainless steel plate. The plate is tightened to the Kimax flange on the bottom of the column.

The column, when held vertically with the help of clamps in a steel frame, serves as a container for the continuous phase liquid through which liquid drops fell. The windows in the column provide access for photographing the falling drops without introducing distortions in the pictures.

Buret. 'B' is a 50 milliliter buret which has a straight tip with a flange instead of the usual stopcock. The flange is made to hold a Teflon needle valve (described below). The buret is clamped above the glass column along the axis. The dispersed phase liquid is stored in

the buret; the volume of drops discharged into the continuous phase can be read on the buret.

Needle Valve. A Manostat Teflon needle valve 'V' is used. As described above it is attached to the lower tip of the buret, the other end of the valve holds the various size nozzles. The function of the valve is to control the flow rate of the dispersed phase into the nozzle and thus control the rate of drop formation.

Nozzles. Two types of nozzles were used: (1) hypodermic needles of sizes 15, 16, 18, 20, 23 and 27; (2) self-made glass nozzles of different throat sizes. The back end of the glass nozzles was shaped into a small flange to fit the needle valve.

Camera. A 35 mm Nikkorex F camera with 55 mm, f/2 lens, was used for photographing the drops.

Light Source. A 300 watt Westinghouse Movie Flood Lamp in a reflector was used as a light source. Ordinary white air-mail writing paper was placed in front of the reflector to form a light diffuser. Two plastic polaroid sheets 6" x 6" were placed on both sides of the column windows to get better contrast in the picture for some systems.

While using the polaroids it was thought that a polarized beam of light would illuminate the continuous liquid media, and the portion of the beam striking the droplet would be deflected. Therefore, when the droplet was viewed through an analyzer it appeared dark compared to the continuous media and gave a better contrast in the picture. This technique of photographing the droplets worked well with three systems:

1. Water - methyl isobutyl ketone
2. Water - hexane
3. Bromobenzene - water

Film. Film used was 400 ASA, Kodak Tri X.

Stop Watch. A stop watch of accuracy 0.05 seconds was used in conjunction with the drop velocity measurements.

Miscellaneous. Reynold's Aluminium Foil and Saran Rap were frequently used to cover the top of column and buret. This was done to minimize the contamination of the liquids by dust particles. Saran-Rap and aluminium foil were also used to seal the one gallon liquid storage containers.

F. Experimental Procedure

The procedure followed in the experiments is described below:

1. All the glass apparatus were washed with hot chromic acid and rinsed with laboratory distilled water before use.
2. The glass column was clamped vertically in a steel support and filled with the continuous phase liquid up to about half inch from the top of the column.
3. The buret was filled with the dispersed phase liquid and clamped above the column. The proper size nozzle was attached to the needle valve, and the buret was lowered so that the tip of the nozzle was about one centimeter below the surface of the continuous phase liquid.
4. The light source was placed about ten inches behind the column window.
5. The camera was fixed on a tripod two feet away from the column axis and focused on a glass rod placed inside the column.
6. The shutter in the camera was set at 0.001 seconds for all the cases. The lens aperture was adjusted by trial and error to find the

correct aperture setting.

7. The needle valve was opened, and the frequency of drop formation was adjusted to about ten to fifteen drops per minute. During each run the frequency of drop formation was checked four or more times. No appreciable change in frequency of formation was noticed.
8. In order to calculate the volume of a drop, buret readings at the beginning of a run and at the end of a run were recorded along with the total number of drops formed during the run. It was assumed that all the drops formed had the same volume.
9. In order to calculate the droplet fall velocity, the falling drops were timed with a stop watch between two markings on the column. The upper and lower markings in all the cases were at least 15 cm from the top and bottom ends of the column, respectively. This was done to avoid end effects. Hence, the fall height used to calculate the droplet velocities was about 50 cm. During each run 20 or more drops were timed for calculating the velocity.
10. During a run three individual drops were photographed. The first photograph was taken

at the start of the run; the second photograph was taken almost at the middle of the run; and the third photograph was shot near the end of the run.

Operations 8, 9 and 10 were performed during each run.

11. The exposed film was developed, and the negative was cut into individual frames and mounted on 2 x 2 inch Kodak Ready Mounts.
12. These transparencies were projected through a slide projector on to a paper sheet hooked on a wall. The outline of the drop's image on the paper was then traced with pencil. Horizontal and vertical drop diameters were recorded from the above drawings.

G. Calculations

The recorded data were used to calculate the following three quantities:

- (1) Drop velocity
- (2) Equivalent drop diameter
- (3) Eccentricity

Drop Velocity.

$$\begin{aligned}
 U_t &= \frac{\text{Distance}}{\text{Average time of fall}} \\
 &= \frac{S}{\frac{1}{N} \sum_{n=1}^N t_n} = \text{cm/sec} \quad (3.1)
 \end{aligned}$$

Equivalent Drop Diameter.

Average volume of a drop = $\frac{\text{Total volume change in the buret}}{\text{Number of drops formed}}$

$$V = \frac{V}{N} = \text{ml}$$

$$\text{Equivalent drop diameter, } d_e = \left(\frac{6}{\pi} V\right)^{1/3} = \text{cm} \quad (3.2)$$

Eccentricity.

Eccentricity, $E = \frac{\text{Horizontal diameter}}{\text{Vertical diameter}}$

$$E = \frac{a}{b}$$

Average eccentricity, E , of any drop size was obtained by taking the average of the three observations,

$$E = \frac{E_1 + E_2 + E_3}{3} \quad (3.3)$$

All calculations were made using an IBM 1620 computer, and the velocity, equivalent diameter and eccentricity of drops are listed in appendix B.

H. Results

The calculated results are tabulated in appendix B. In the next chapter these results will be analyzed.

Data on the benzyl alcohol - hexane system could not be obtained because benzyl alcohol formed a jet spray in hexane; even the smallest size nozzle failed to form individual droplets. Therefore, it was impossible to measure velocity and volume of individual drops.

Two other systems which failed to yield data are water in benzene and glycol in methyl isobutyl ketone. In these two cases all attempts failed to produce sharp photographs of the droplets.

IV. DISCUSSION

As is indicated in the literature review section, no satisfactory method is currently available to predict the deformation of liquid drops moving in liquid media. In this study, special attention has been given to obtaining drop deformation data on the systems which cover a wide range of physical properties. The data reported in the literature which is presented in appendix B cover a very limited range with regard to continuous phase viscosity ($\mu_c = 0.89$ to 1.56 c.p.). This work includes systems with continuous phase viscosity as low as 0.31 centipoise and as high as 45.93 centipoise. While the data analysis for the present work was under way, a set of additional data was received from Dr. A.H. P. Skelland of Notre Dame University. The data are included in appendix B.

A. Data from Literature

Only a selected portion of the literature data has been used in this study, in addition to the data obtained in this project. All the data selected are for non-oscillating drops. The three key variables which

were examined were the equivalent droplet diameter, terminal velocity and eccentricity. Since most authors have not indicated whether or not the droplets were oscillating, it was necessary to devise a method for determining which droplets oscillate so that eccentricity data for oscillating droplets could be discarded. The data selection from literature is explained below.

Klee (12): The terminal velocity, U_t , versus equivalent droplet diameter, d_e , plots for the nine systems were constructed using all the data of the author. Drop diameters corresponding to the peak velocities were recorded. Data having a diameter equal to or larger than the peak velocity diameter for a particular system were rejected because those droplets were probably oscillating. In cases where the peak velocity was not very obvious, personal judgement was used. Of the one hundred and four data points, thirty seven were rejected as possibly being oscillating droplet data.

Garner and Tayeban (6): Data available for the two systems in this case were physical properties of the systems, equivalent drop diameters, eccentricities, and the corresponding Reynolds numbers. First, velocities of the drops were back-calculated from the Reynolds

numbers ($U_t = Re/\mu_c/d_e\rho_c$). Then, a procedure similar to above was used for data selection. Of the seventeen data points, eleven were rejected as possibly being oscillating droplet data.

Keith and Hixson (11): Equivalent drop diameters corresponding to the peak velocities of the six systems were read directly from their U_t versus d_e plots. Peak velocity diameters were then marked for each system on the eccentricity versus equivalent diameter plots. Values of d_e , U_t and E for non-oscillating drops were read from these plots. The equivalent diameter versus eccentricity plot is given in the appendix B.

Wellek (24): equivalent diameter, terminal velocity and eccentricity data for six systems were available. Half of the systems were mutually saturated, and half were unsaturated. Of the thirty five data points, fifteen were rejected as possibly being oscillating droplet data.

Skelland (22): equivalent diameter, terminal velocity and eccentricity data for fourteen systems were available. The data received were analyzed as in the first case and data for non-oscillating drops selected. Of the eighty data points, thirty two were rejected as possibly being

oscillating.

B. Regression Analysis

The eccentricity of droplets is a function of many variables,

$$E = f(d_e, U_t, g, \sigma_i, \mu_c, \mu_d, \rho_c, \Delta \rho) \quad (4.1)$$

The object of this investigation is to determine the above functional relation. Attempts to derive a correlation between the variables from an assumed theoretical model have not been successful (7). One approach to the solution of such a difficult problem is the method of correlation by dimensional analysis. It can be shown that the above relation may be reduced to the following relation by dimensional analysis:

$$E = f_2\left(\frac{d_e U_t^2 \rho_c}{\sigma_i}, \frac{d_e U_t \rho_c}{\mu_c}, \frac{g \Delta \rho d_e^2}{\sigma_i}, \frac{U_t^2}{g d_e}, \frac{\mu_c}{\mu_d}\right) \quad (4.2)$$

or identifying the dimensionless groups symbolically

$$E = f_2\left(We, Re, E\delta, Fr, \frac{\mu_c}{\mu_d}\right) \quad (4.3)$$

The number of independent variables in the functional relation has been reduced from eight in equation (4.1) to five in equation (4.3). The functional relation f_2 , however, is still unknown. In this work, f_2 , is assumed to have an exponential form.

$$E = a_0' We^{a_1'} Re^{a_2'} Eö^{a_3'} Fr^{a_4'} \left(\frac{\mu_c}{\mu_d}\right)^{a_5'} \quad (4.4)$$

Inspection of the above relation indicates a serious deficiency. It is well known that as either d_e or U_t approaches zero (and hence, We , Re , $Eö$, and Fr approach zero), the droplet eccentricity, E , should approach unity. Equation (4.4), however, suggests that the eccentricity approaches zero. Therefore, equation (4.4) was further modified to the following form

$$E = a_0 We^{a_1} Re^{a_2} Eö^{a_3} Fr^{a_4} \left(\frac{\mu_c}{\mu_d}\right)^{a_5} + 1.0 \quad (4.5)$$

$$\text{or } E^* = (E-1.0) = a_0' We^{a_1'} Re^{a_2'} Eö^{a_3'} Fr^{a_4'} \left(\frac{\mu_c}{\mu_d}\right)^{a_5'} \quad (4.6)$$

The constants in the above relation were determined by means of a multiple regression analysis program outlined by M.A. Efrymson (3). This program is listed in the University of Missouri, Rolla Computer Science Center as STST04. The program uses a modified least square technique. Equation (4.6) must first be linearized by a logarithmic transformation as follows:

$$\begin{aligned} \ln(E-1) = \ln(a_0') + a_1' \ln(We) + a_2' \ln(Re) + a_3' \ln(Eö) \\ + a_4' \ln(Fr) + a_5' \ln\left(\frac{\mu_c}{\mu_d}\right) \end{aligned} \quad (4.7)$$

The regression analysis program is such that it does not fit the experimental data to all of the five independent variables. It first searches for the independent

variable, for example $\ln(We)$, which has the most important effect on $\ln(E-1)$. The first correlation would then be

$$\ln(E-1) = \ln(a'_0) + a'_1 \ln(We) \quad (4.8)$$

The program gives the standard error of the correlation, $S[\ln(E-1)]$, the value of $\ln(a'_0)$ and a'_1 , and also the standard error of the coefficient a'_1 (from which the ninety five percent confidence limits of a'_1 are determined).

The program is such that the next step is a search for the second most important variable, say $\ln\left(\frac{\mu_c}{\mu_d}\right)$.

A second correlation would then be obtained

$$\ln(E-1) = \ln(a''_0) + a''_1 \ln(We) + a''_2 \ln\left(\frac{\mu_c}{\mu_d}\right) \quad (4.9)$$

The process is continued automatically until a point is reached where with the effect of additional variables on the correlation is statistically insignificant or all of the independent variables are introduced.

Two functions directly involving the primary variables were analyzed using the regression analysis program. They are:

$$E^* = E-1 = a_0 d_e^{a_1} U_t^{a_2} \sigma_i^{a_3} \mu_c^{a_4} \mu_d^{a_5} R_c^{a_6} \Delta \rho^{a_7} \quad (4.10)$$

$$E^* = E-1 = b_0 d_e^{b_1} \sigma_i^{b_2} \mu_c^{b_3} \mu_d^{b_4} R_c^{b_5} \Delta \rho^{b_5} \quad (4.11)$$

Equation (4.11) was studied because it does not employ

the terminal velocity, U_t , and may be used for a quick estimate of eccentricity. Also it should be recalled that U_t is a function of all the other independent variables.

The following function was also studied

$$E^* = E-1 = c_0 E_0 \quad (4.12)$$

An ordinary regression analysis program was used for this simple linear function.

After the constants in each function were determined by the regression analysis programs, the average absolute percentage deviation* of the calculated eccentricities from the experimentally observed eccentricities was determined for each correlation. The lower the average absolute percentage deviation for a correlation, the more desirable the correlation becomes.

Five correlations which are probably the most useful are listed in Table II, page 62. Correlation number II is due to Harmathy and was not developed in this investigation.

$$* \text{ A.A.P.D.} = \frac{100}{N} \sum_1^N \frac{|E_{\text{cal}} - E_{\text{obs}}|}{E_{\text{obs}}}$$

C. Results

The following five correlations were obtained by regression analysis of two hundred and eight data points representing forty five systems:

$$E = 1.0 + 0.123E\delta \quad (4.13)$$

$$E = 1.0 + 0.089 \sigma_i^{0.82} d_e^{1.92} \Delta\rho^{0.79} \mu_c^{-0.44} \mu_d^{-0.11} \quad (4.14)$$

$$E = 1.0 + 0.091We^{0.95} \quad (4.15)$$

$$E = 1.0 + 0.092We^{0.98} (\mu_c/\mu_d)^{0.06} \quad (4.16)$$

$$E = 1.0 + 0.137U_t^{1.81} \sigma_i^{-0.97} d_e^{1.07} \mu_d^{-0.08} \quad (4.17)$$

The graphical solution of Harmathy for predicting eccentricity of the drops or bubbles is shown in Figure 12.

An analytical relation

$$E = 0.815 + 0.22E\delta - 5.3 \times 10^{-3} E\delta^2 + 4.47 \times 10^{-5} E\delta^3 \quad (4.18)$$

was obtained by carefully fitting a third order polynomial to the curve in Figure 12 by least squares curve fitting techniques.

The average absolute percentage deviation, defined as

$$A.A.P.D. = \frac{1}{N} \left(\sum_{i=1}^N \frac{|E_{obs} - E_{call}|}{E_{obs}} \right) 100 \quad (4.19)$$

was also calculated using the two hundred and eight data points for all the above correlations and are listed in Table II. The 95 percent confidence limits of the important constants are also listed.

In addition to the regression analysis programs used, an attempt was made to graphically correlate the data. After considerable trial and error, a plot of $\ln(E \cdot Re)$ against $\ln(E_o \cdot We)$ resulted in a set of parallel straight lines. (See Figure 24, page 109.) In the figure, each straight line represents a system. The slope, of the straight lines are approximately 0.5.

D. Discussion of Results

Eccentricity data from a total of forty five liquid-liquid systems have been studied, covering a wide range of physical properties. Out of forty five systems, ten systems were experimentally studied in the present work, and the data on the remaining thirty five systems were obtained from literature or elsewhere*.

* Dr. A.H.P. Skelland

Dr. R.M. Wellek

TABLE II

Correlations 1 through 6 with 95 Percent Confidence Limits of Key Parameters

Correlation No.		Average Absolute Percent Deviation
1.	$E = 1.0 + 0.123E\ddot{o}$ 0.123 ± 0.000046	7.8
2.	$E = 0.815 + 0.22E\ddot{o} - 0.0053E\ddot{o}^2 + 4.47 \times 10^{-5} E\ddot{o}^3$	13.6
3.	$E = 1.0 + 0.089 \sigma_i^{0.823} a_e^{1.92} \Delta\rho^{0.79} \mu_c^{0.441} \mu_d^{-0.114}$ $-0.823 \pm 0.106; 1.92 \pm 0.26; 0.79 \pm 0.14$ $-0.441 \pm 0.12; -0.114 \pm 0.06$	7.4
4.	$E = 1.0 + 0.091W_e^{0.953}$ 0.0953 ± 0.084	6.2
5.	$E = 1.0 + 0.092W_e^{0.984} (\mu_c/\mu_d)^{0.063}$ $0.984 \pm 0.084; 0.063 \pm 0.04$	6.0
6.	$E = 1.0 + 0.137U_t^{1.81} \sigma_i^{-0.97} a_e^{1.07} \mu_d^{-0.078}$ $1.81 \pm 0.18; -0.97 \pm 0.088; 1.07 \pm 0.16;$ -0.078 ± 0.046	5.9

The range of physical properties of the systems and certain important dimensionless groups covered in this study are given in Table III.

The five new correlations obtained in this work and the Harmathy relation (correlation 2) for predicting the eccentricity of liquid drops in liquid media are discussed here in detail. The average percentage deviation for correlations 1, 2, 3, 4, 5, and 6, is 7.8, 13.6, 7.4, 6.2, 6.0 and 5.9, respectively. The correlations obtained in this work are a significant improvement over the Harmathy correlation (number 2). The values of the exponents of correlations 3, 4, 5, and 6 are analyzed in Table II where the ninety five percent confidence limits of the exponents are given.

Correlation 6 gives the smallest average percentage deviation, and judged on this basis it is the best correlation for predicting drop eccentricity. However, the difference in average percentage deviation between correlations 4, 5 and 6 are not large. The constants and exponents on the Weber group in correlations 4 and 5 are essentially the same, but correlation 5 has an extra dimensionless group (μ_c/μ_d).

TABLE III

Range of Physical Properties of the Systems and Certain Important Dimensionless Groups Covered in this Study

Variable	Symbol	Range	Units
Interfacial tension	σ	0.30 to 42.4	dynes/cm
Continuous phase viscosity	μ_c	0.31 to 45.9	centi-poises
Dispersed phase viscosity	μ_d	0.48 to 85.0	centi-poises
Continuous phase density	ρ_c	0.6655 to 1.1995	gm/ml
Dispersed phase density	ρ_d	0.7723 to 1.6740	gm/ml
Reynolds number	Re	5.29 to 1354	none
Weber number	We	0.16 to 12.58	none
Eötvös number	Eö	0.14 to 10.10	none
Viscosity ratio	μ_c/μ_d	0.011 to 53.4	none

$$E = 1.0 + 0.091 We^{0.95} \quad \text{cor. 4}$$

$$E = 1.0 + 0.092 We^{0.98} (\mu_c/\mu_d)^{0.06} \quad \text{cor. 5}$$

The exponent on the group (μ_c/μ_d) is 0.06 which is quite small. Therefore, $(\mu_c/\mu_d)^{0.06}$ could be approximated by 1.0 if the viscosity ratio is close to unity. However, the effect of the viscosity group can not be neglected when the viscosity ratio is very large or very small, as it is, for example, for the diol-water system ($\mu_c/\mu_d = 0.011$) studied by Garner and Tayeban (6) or the water-corn oil system ($\mu_c/\mu_d = 53.4$) studied in this work.

Correlation 6 also is similar to correlation 4 except for the constants;

$$\begin{aligned} E &= 1.0 + 0.137 U_t^{1.81} \sigma_i^{0.97} d_e^{1.07} \mu_d^{-0.08} \quad \text{cor. 6} \\ &\cong 1.0 + 0.137 U_t^{2 \times 0.95} \sigma_i^{0.95} d_e^{0.95} \mu_d^{-0.08} \\ &\cong 1.0 + 0.137 U_t^{2 \times 0.95} \sigma_i^{-0.95} d_e^{0.95} \times 1.0 \\ &\cong 1.0 + 0.137 We^{0.95} \quad (4.20) \end{aligned}$$

Since, correlation 4 is essentially the same as correlation 5 or 6, 4 could be selected favorably for use for its simplicity over the 5 or 6 without introducing serious error in the results. Correlation 5 would be recommended if viscosity ratios are encountered which differ significantly from unity. If one does not wish to calculate

the terminal velocity in order to calculate the eccentricity, then correlation 3 is recommended.

1. Comparison of the Correlations. Figures 16, 17, 18, and 19 are plots of calculated eccentricities against observed eccentricities for correlations 1, 2, 3 and 4, respectively. The deformation of drops is arbitrarily divided into three categories

Less deformed drops	$1.0 < E < 1.2$
Moderately deformed drops	$1.2 < E < 1.5$
Highly deformed drops	$1.5 < E$

Less deformed drops ($1.0 < E < 1.2$). Eccentricities calculated from correlations 1, 3, and 4 are in good agreement with the observed eccentricities; correlation 3 and 4 agree very well (see Figure 16, 18 and 19). Correlation 1 gives slightly lower values than the observed values of the eccentricity. Correlation 2 (that of Harmathy) is not satisfactory for the lower region of deformation (see Figure 17). The calculated values are much lower than the observed values. Harmathy's correlation has another serious disadvantage; the calculated eccentricity quite often is less than 1.0 which is impossible (unless wall effects are important).

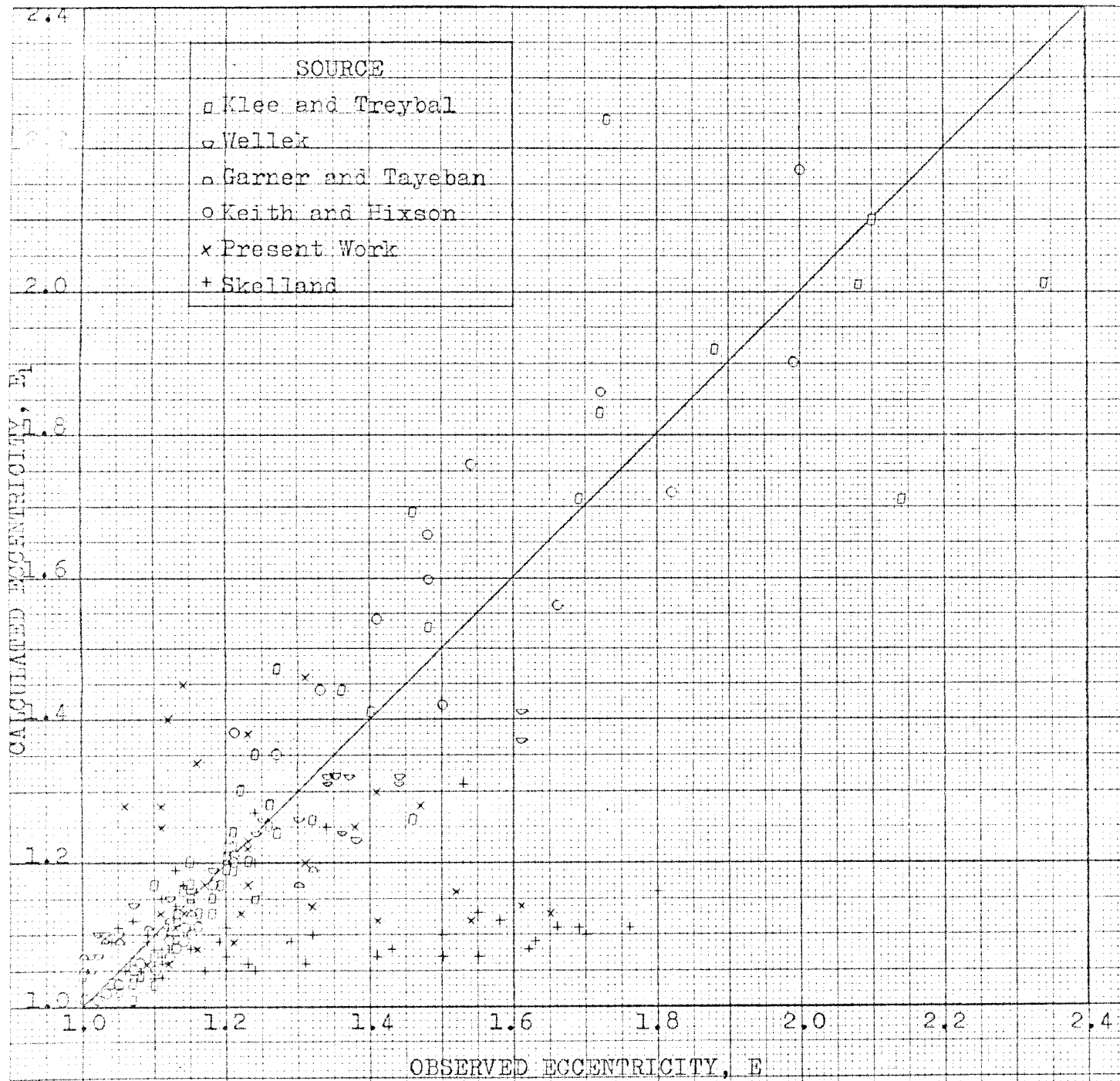


Figure 16. Comparison of observed eccentricity with those calculated from correlation no. (1) for all data points

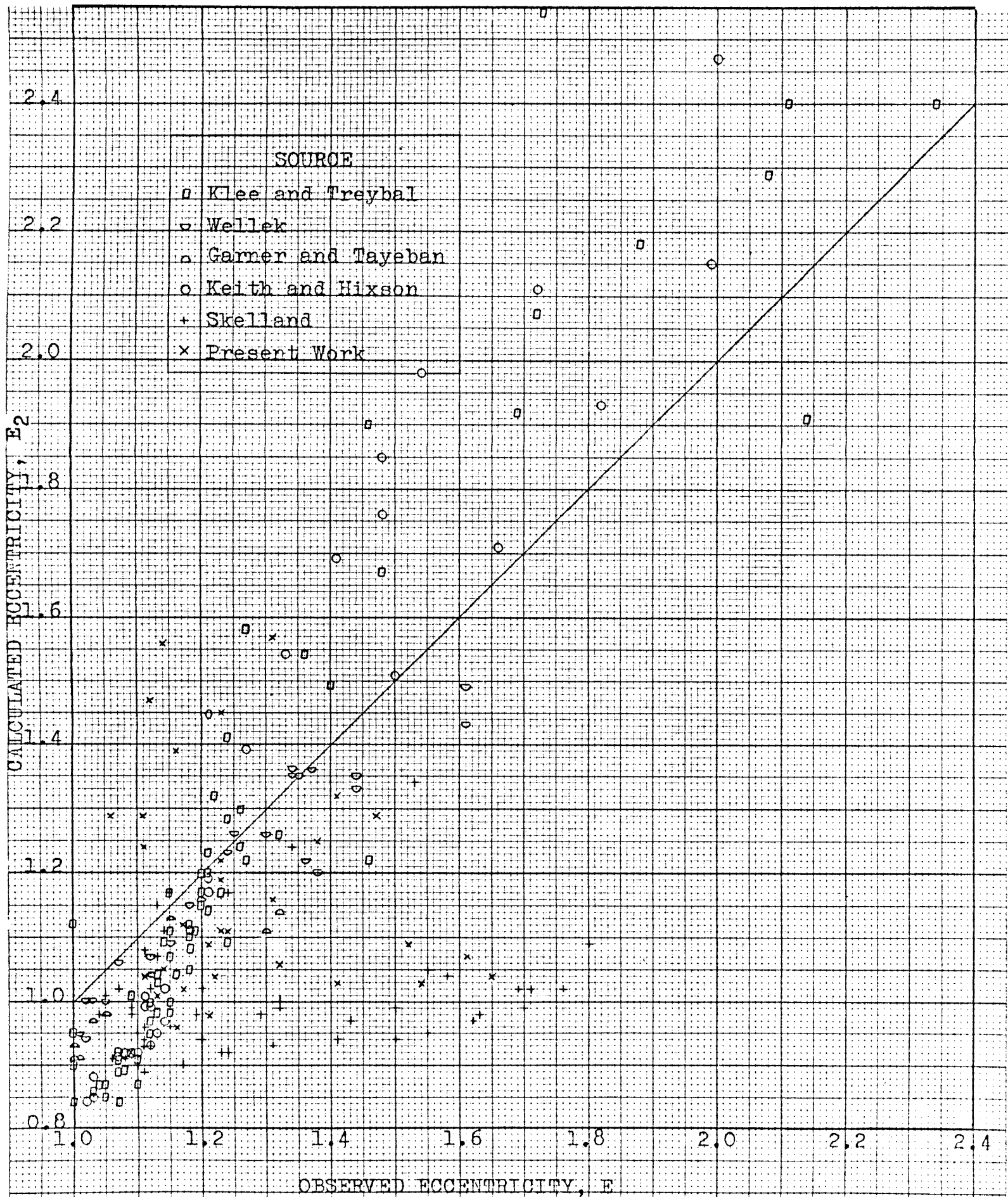


Figure 7. Comparison of observed eccentricity with those calculated from correlation no. (2) for all data points (Harmathy's correlation)

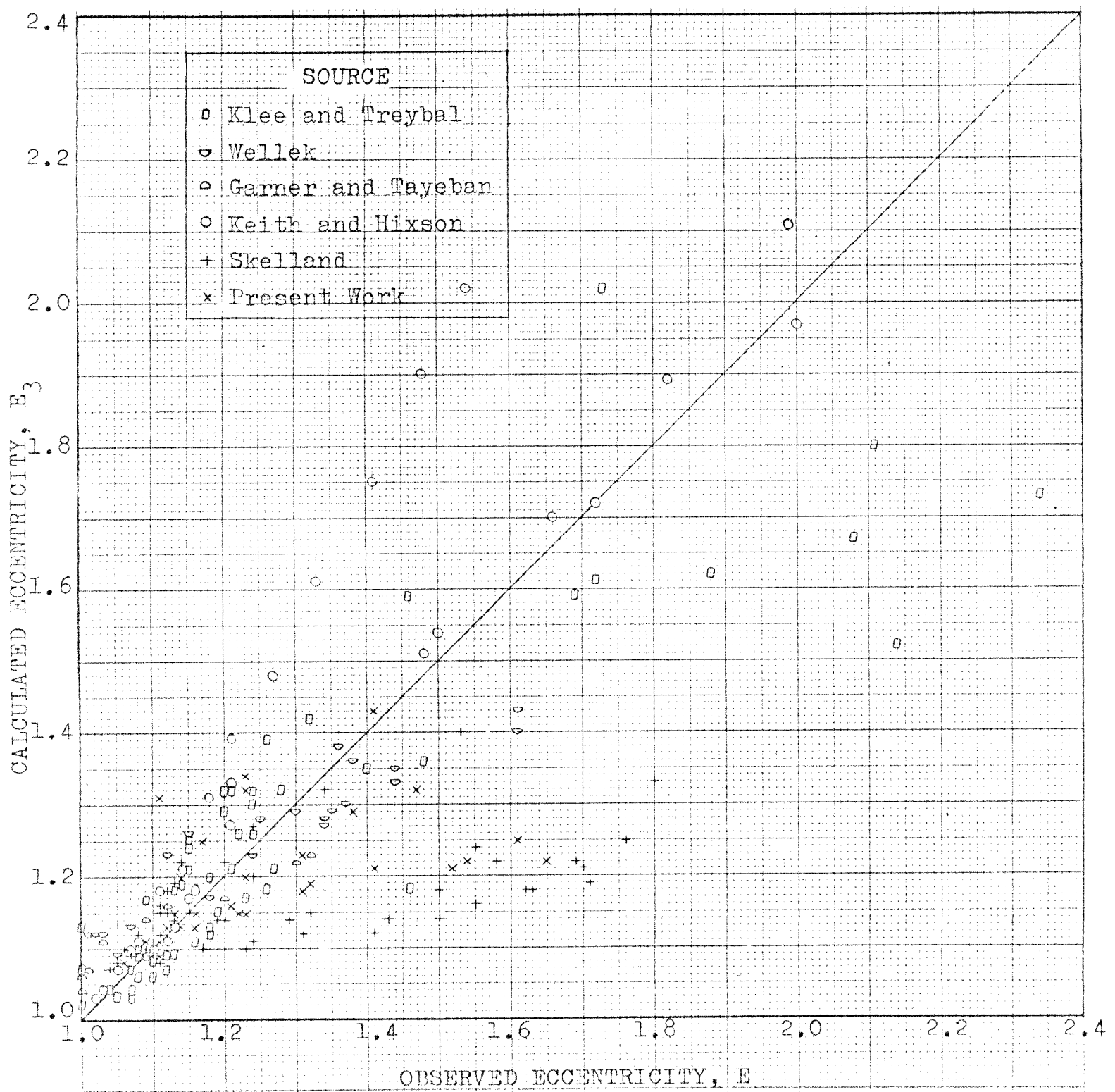


Figure /8. Comparison of observed eccentricity with those calculated from correlation no.(3) for all data points

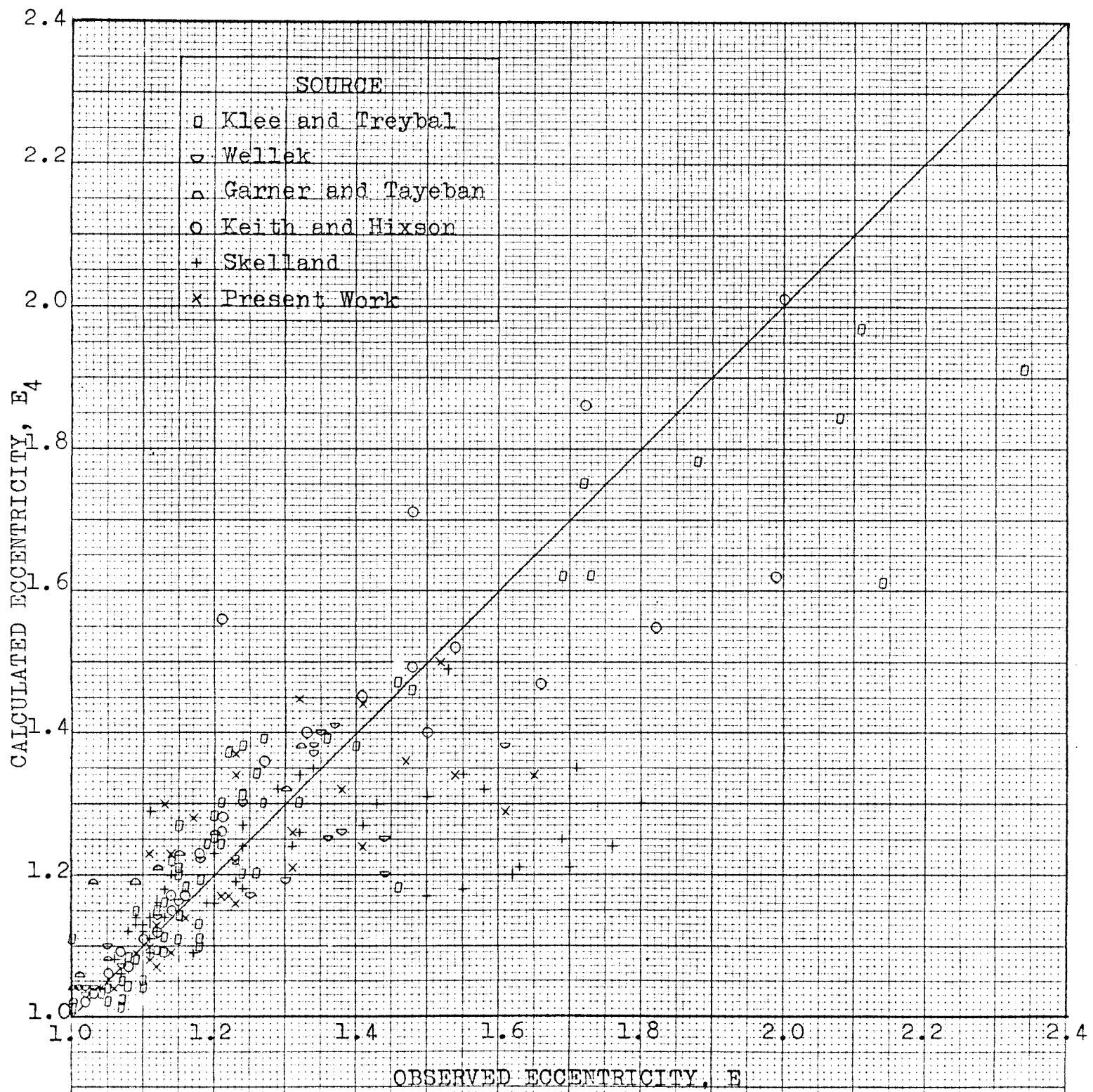


Figure 19. Comparison of observed eccentricity with those calculated from correlation no. (4) for all data points

Moderately deformed drops ($1.2 < E < 1.5$). Deformation in the region is best predicted by correlation 4 (see Figure 19). Deviations in the predicted value are slightly more than in the low deformation region. Correlations 1 and 3 show identical behavior, and the deviation in calculated values of eccentricity for both the correlations is higher than for correlation 4. Harmathy's correlation 2 is poorer in accuracy than the other three correlations.

It can be seen from Figures 16 to 19 that a large number of points from the data of Skelland (22) show a definite pattern on all four graphs; the observed values are very high compared to the values calculated by any of the correlations. It is possible that some of the data of Skelland may be in error.

Highly deformed drops ($E < 1.5$). In this region of deformation accuracy is poor for all of the correlations. Of the four developed in this work, correlation 1 seems to give the best results. Correlation 2 (Harmathy) predict values higher than those observed. Correlation 3 does not show any particular trend, but the deviation from observed values is large. The values of eccentricity calculated from correlation 4 in general are lower than the observed values.

2. Effect of Equivalent Drop Diameter on Eccentricity. It is well known that the greater the drop size, the greater the eccentricity, i.e., deformation. Previous workers Klee and Treybal (13), Keith and Hixson (11), and Garner and Tayeban (6) have suggested that the eccentricity, E_e , of drops is a linear function of the equivalent drop diameter, d_e (see Figures 7, 8, 9). They frequently did not separate their data into oscillating and non-oscillating regions when they prepared their plots of eccentricity data. Studies by Elzinga and Banchemo (4) of pure and contaminated water drops in Dowtherm A+E show that eccentricity is not a linear function of the equivalent drop diameter. Klee and Treybal, however, had pointed out that the eccentricity of small drops is not strictly linear with respect to equivalent drop diameter.

In Figures 20, 21, and 23, the observed eccentricities and those calculated from correlations 1, 2, 3, and 4 have been plotted against equivalent drop diameter for a number of systems. From these figures, it is clear that eccentricity of drops is not exactly linear with respect to equivalent drop diameter. Correlations 1 and 3 represent the trend of the observed data fairly well in all three figures. Equivalent drop diameter, d_e ,

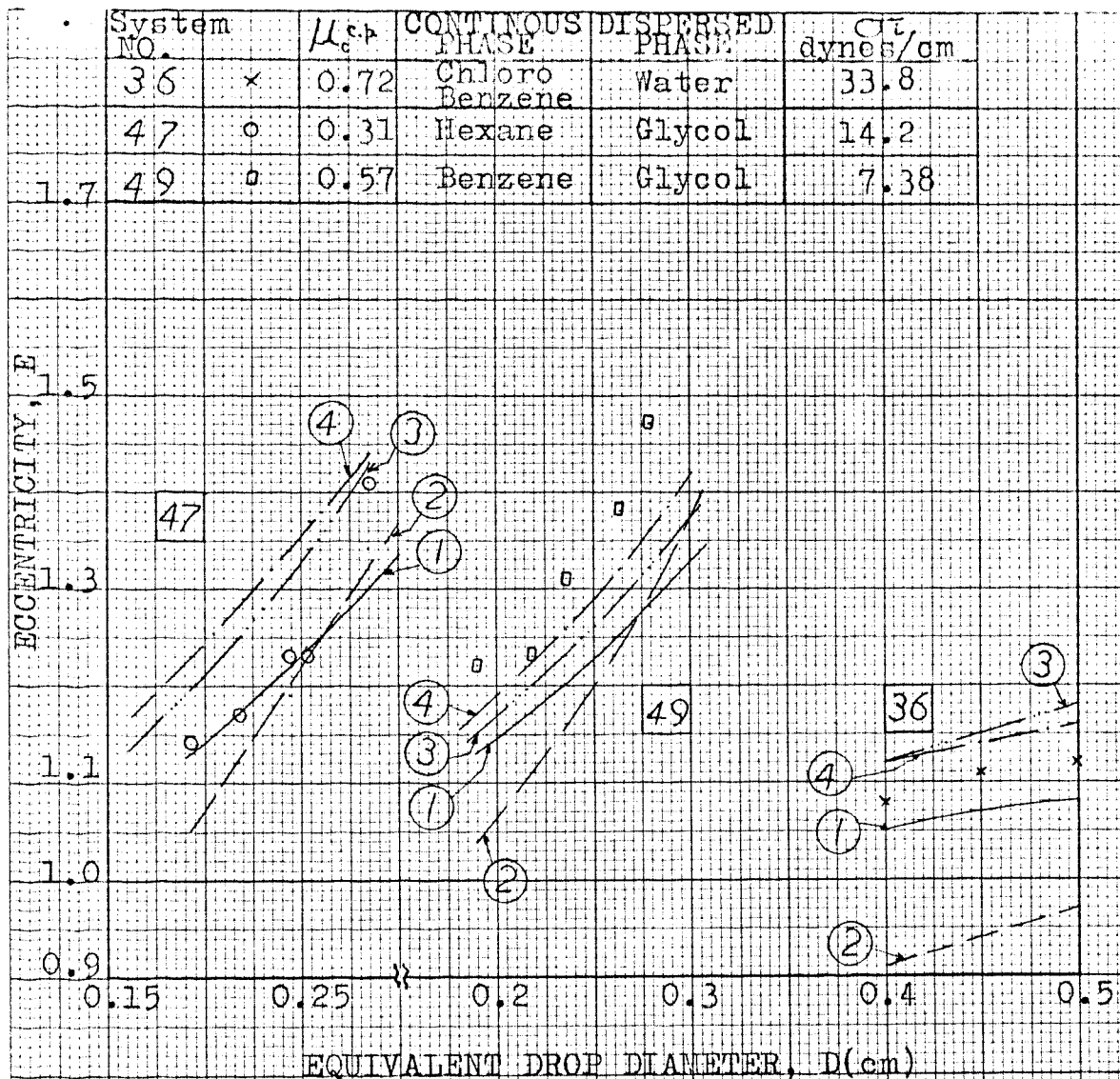


Figure 20. Observed eccentricity and calculated eccentricity as a function of equivalent drop diameter "in the 0.31 to 0.72 c.p. μ region"

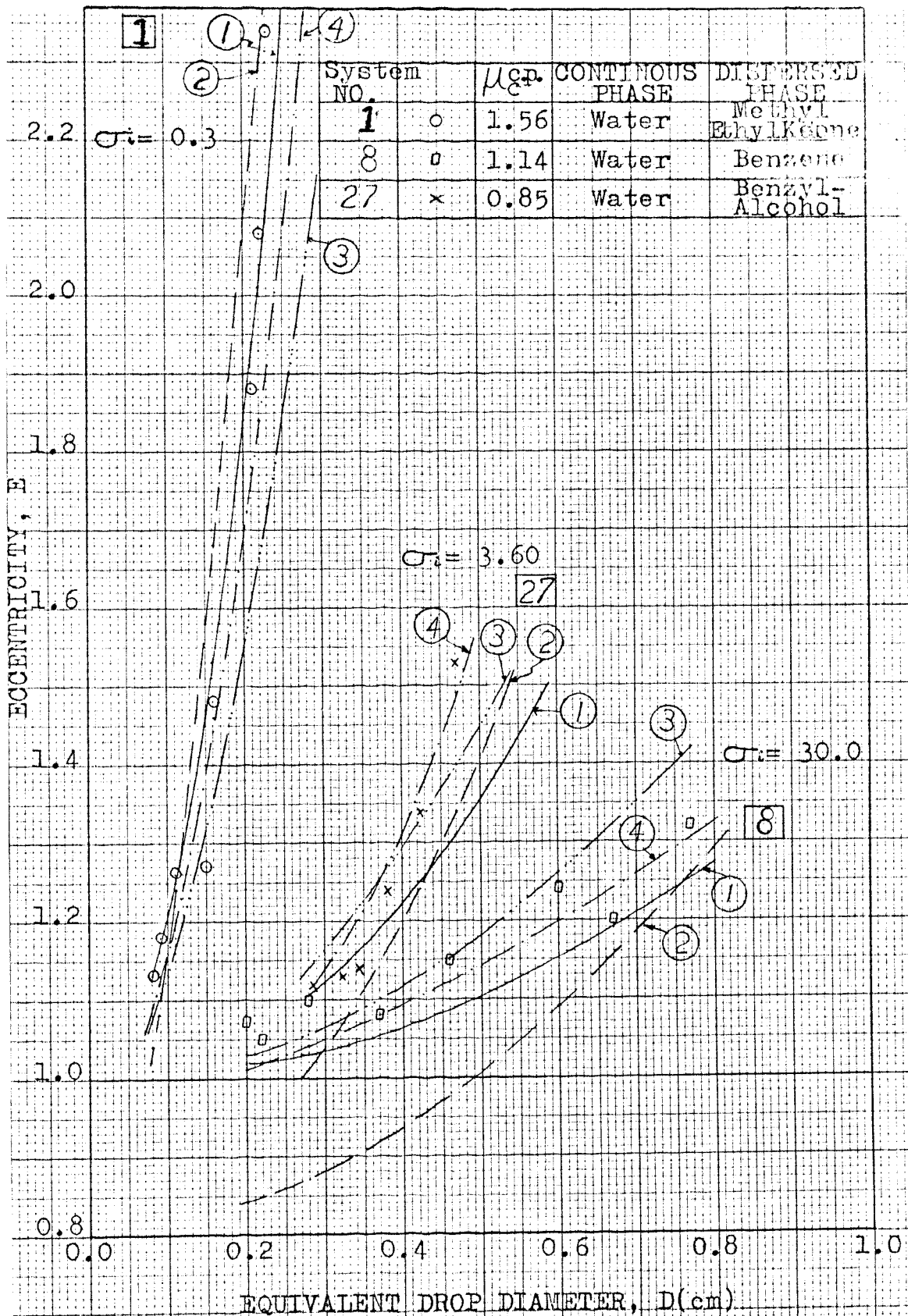


Figure 2%. Observed eccentricity and calculated eccentricity as a function of equivalent drop diameter "in the 0.85 to 4.0 c.p. μ_c region"

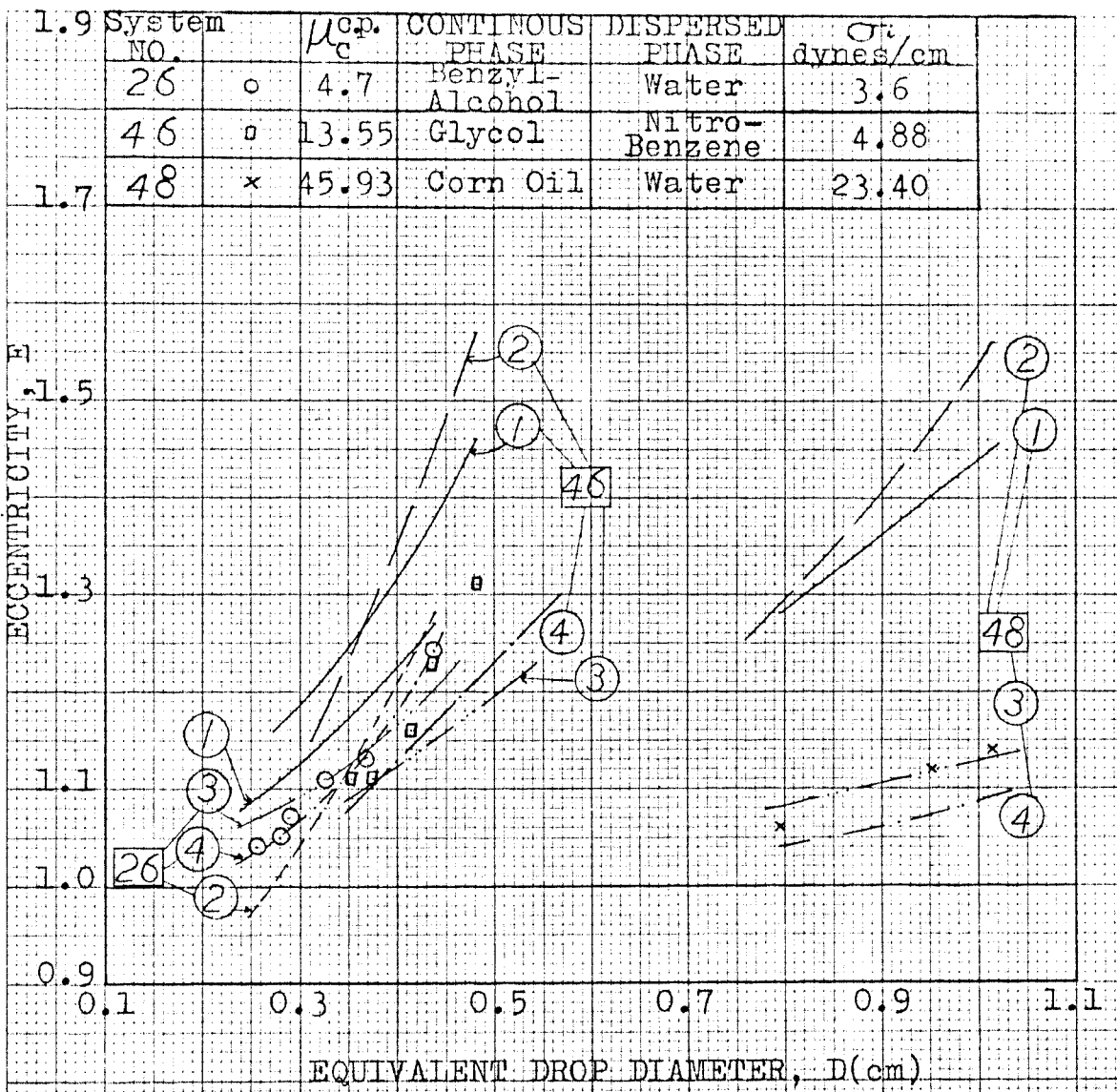


Figure 22 Observed eccentricity and calculated eccentricity as a function of equivalent drop diameter "in the 4.7 to 45.93 c.p. μ_c region"

appears with the following exponents in the correlations 1 and 3:

$$\text{correlation 1: } E \propto d_e^2$$

$$\text{correlation 3: } E \propto d_e^{1.92}$$

Therefore, it is reasonable to assume that for non-oscillating drops, E is proportional to d_e^2 and not $d_e^{1.0}$ as has been reported in the literature. Correlation 4 also represents the data fairly well in all three figures. Since, correlation 4 contains a velocity term, U_t , which is itself a function of d_e , it is difficult to interpret the effect of d_e .

3. Effect of Physical Properties on Eccentricity.

The effect of various physical properties will be discussed, if possible, with all other physical properties the same except the one being considered. This is not always possible, even with the many systems experimentally studied in this work.

Interfacial tension. Interfacial tension was found to be the most important of all physical properties affecting the shape of the drops. The tendency of interfacial forces is to reduce the surface area of the liquid drop to its minimum. For a given volume, a sphere offers the minimum surface area. Therefore, the natural shape

of a liquid droplet not subjected to any other forces is expected to be spherical, i.e., with an eccentricity of unity. Very small drops have been observed to be almost perfectly spherical despite their motion through the continuous phase.

The quantitative dependence of eccentricity on interfacial tension can be judged by considering the magnitude of the exponents of ' σ_i ' in the various correlations:

1. $E \propto \sigma_i^{-1.0}$
2. $E \propto \sigma_i^{-1.0}$
3. $E \propto \sigma_i^{-0.82}$
4. $E \propto \sigma_i^{-0.95}$

This suggests that eccentricity is almost inversely proportional to interfacial tension, i.e., $E \propto 1/\sigma_i$.

Density. The effect of the density ρ_c and ρ_d , on the shape of drops moving in liquid media appears in two ways. The first effect is related to the gravitational forces on the drop causing the motion, and the second is related to the inertial forces opposing the motion. The two forces are represented in the dimensionless groups $E\ddot{o}$ and We , respectively.

$$Eö = \frac{g|\rho_c - \rho_d|d_e^2}{\sigma_i} = \frac{\text{gravitational forces}}{\text{surface forces}}$$

$$We = \frac{\rho_c d_e U_t^2}{\sigma_i} = \frac{\text{inertial forces}}{\text{surface forces}}$$

Correlation 1 and 2 show that drop eccentricity is a function of $Eö$ raised to the unit power. Correlation 2 can be approximated by $E = 0.815 + 0.22Eö$, by neglecting the higher powers of $Eö$, since their coefficients are very small. This suggests that drop eccentricity is directly proportional to $\Delta\rho$, the difference in densities between the two liquids. However, the exponent on $\Delta\rho$ in correlation 3 is not 1.0 but 0.79. Thus,

$$E \propto (\Delta\rho)^x$$

where $x = 0.9$. This is in contrast to the observation of Klee and Treybal (13) that

$$E \propto (\Delta\rho)^{0.5}$$

The individual density term ρ_c appears in the correlations in association with the terminal velocity term, U_t . Correlations 1, 2 and 3 do not have ρ_c terms.

The effect of the individual densities ρ_c and ρ_d on deformation can not be explicitly seen. Correlations 4 or 5 and 6 have the ρ_c term along with the terminal

velocity term, U_t . Since, terminal velocity itself is a function of a host of variables, one of which is ρ_c , it is difficult to explain the effect of ρ_c on eccentricity

Viscosity (Continuous Phase). Harmathy (7) has shown, page 30, that

$$\text{shape} = f_1(E\ddot{o}, We)$$

and when droplets are in turbulent flow region the Weber group becomes a function of Eötvös group, and hence

$$\text{shape} = f_3(E\ddot{o})$$

Correlations 1, 2, and 4 support the above simplified model. Neither $E\ddot{o}$ nor We contain the continuous phase viscosity term. This might suggest, therefore, that the shape or eccentricity of liquid drops is not affected by the continuous phase viscosity. However, correlations 3 and 5 do contain the continuous phase viscosity term, μ_c . The exponent on μ_c , in correlation 5 is small, 0.06, and suggests that the effect of μ_c on eccentricity is almost negligible. In correlation 3, the exponent on μ_c is -0.44 indicating that the effect of μ_c is significant.

The following is an analysis of the various correlations in different ranges of continuous phase viscosity. In Figures 20, 21, and 22, the observed eccentricity and calculated eccentricity using correlations

1, 2, 3, and 4 have been plotted against the equivalent drop diameter for systems having low, medium and high continuous phase viscosities, respectively. The ranges of viscosity have been arbitrarily defined by the author as follows:

Low viscosity range	$\mu_c < 0.8$ c.p.
Medium viscosity range	$0.8 < \mu_c < 4.0$ c.p.
High viscosity range	$4.0 < \mu_c$ c.p.

In Figures 20 and 21, correlations 1, 3 and 4 represent the trend of data fairly well. Figure 22 represents the data of high viscosity systems. Here, correlation 1 shows large deviations from the observed data, and this becomes progressively worse as μ_c increases from system 26 to system 48. Correlations 3 and 4 fall close to the observed data of system 48. Correlation 1 predicts higher eccentricities than those observed for high continuous phase viscosity systems. Correlation 2 of Harmathy is shown to be poor on page 66, and, therefore, is not discussed here.

The failure of correlation 1 to represent the data of high viscosity systems is probably because of the absence of the μ_c term in the correlation. This leads to the tentative conclusion that the effect of continuous

phase viscosity on eccentricity is little so long as the viscosity, μ_c , is less than 4.0 centipoises. In the higher viscosity range ($\mu_c > 4.0$ c.p.), the effect is to lessen the drop deformation. A similar conclusion could be drawn by considering correlation 3, where μ_c is present with an exponent of -0.44.

It would be a mistake to assume that correlation 4 does not include the effect of continuous phase viscosity. This correlation has the Weber group ($We = \frac{\rho_c d_c U_t^2}{\sigma}$) as a dimensionless variable which includes the terminal velocity term, U_t . The terminal velocity is a function of the continuous phase viscosity, and hence, correlation 4 also includes the effect of continuous phase viscosity, though indirectly.

Viscosity (Dispersed Phase). Liquid drops differ from solid spheres in that the liquid can be set into motion internally by the viscous drag in the liquid medium outside the drops. The intensity of circulation inside the drops depends upon the viscosity of the dispersed phase liquid, μ_d . It is natural, therefore, to expect some effect of μ_d on drop shape and any other associated phenomena.

It is the observation of many investigators (8,13) that the terminal velocity of drops is affected very little by the dispersed phase viscosity. Schroeder and Kintner (20) found that oscillation of drops is affected very little by dispersed phase viscosity. Garner and Tayeban (6) report that μ_d effects the magnitude of drop deformation; the eccentricity of highly viscous drops was found to be less than that of less viscous drops. But, as discussed earlier

$$E = f_1(Eö) \quad \text{or} \quad E = f_4(We)$$

which would indicate, if Harmathy's model is correct that eccentricity is not affected by μ_d . However, correlation 3 indicates that the effect of μ_d on eccentricity is very small, $E \propto \mu_d^{-0.11}$. It can be seen from Figures 16, 18 and 19 that correlation 3 does not offer any better results than either correlation 1 or 4 for the Garner and Tayeban data which includes a very high viscosity diol ($\mu_d = 85$ c.p.). Systems 1, 6, 7, and 23 represent the extremes of the dispersed phase viscosity range investigated in this study. The observed and calculated eccentricities, Table VII, show that the eccentricity for these systems calculated using correlation 3 is in no way better than those calculated using correlations 1 and 4.

Therefore, the author's view is that dispersed phase viscosity, μ_d , has very little effect on the shape of a drop.

V. CONCLUSION

Thirteen liquid-liquid systems were experimentally studied in this investigation. Data from the open literature and elsewhere were also included for the theoretical investigation. The following conclusions are drawn from this investigation:

1. An analytical relation

$$E = 0.815 + 0.22E_0 - 0.0053E_0^2 + 4.47 \times 10^{-5} E_0^3$$

was obtained by carefully fitting a third order polynomial to Harmathy's E versus E_0 curve by least squares curve fitting techniques. This correlation when tested with available data, proved unsatisfactory. It occasionally predicted eccentricity values lower than 1.0, which is impossible for non-oscillating drops. The average absolute percentage deviation for the Harmathy correlation was found to be 13.6 percent.

2. Five new correlations were obtained by regression analysis of the data.

1. $E = 1.0 + 0.123E_0$

3. $E = 1.0 + 0.089 \sigma_i^{0.82} d_e^{1.92} \Delta\rho^{0.79} \mu_c^{-0.44} \mu_d^{-0.11}$

$$4. E = 1.0 + 0.091We^{0.95}$$

$$5. E = 1.0 + 0.092We^{0.98} (\mu_c/\mu_d)^{0.06}$$

$$6. E = 1.0 + 0.137U_t^{1.81} \sigma_i^{-0.97} d_e^{1.07} \mu_d^{-0.08}$$

The average absolute percentage deviation of the calculated eccentricities from observed eccentricities for the two hundred and eight data points representing forty five systems is 7.8, 7.4, 6.2, 6.0, and 5.9 percent for correlations 1, 3, 4, 5, and 6, respectively. Correlations 4, 5, and 6 were considered similar. Therefore, only correlations 1, 3, and 4 were studied in detail. It was found that correlation 1 is good only for systems which have low or moderate continuous phase viscosity ($\mu_c < 4.0$ c.p.). Correlations 3 and 4 were applicable in the whole range of continuous phase viscosity covered in this study (0.31 to 45.9 c.p.).

3. Harmathy's dimensionless model for correlating drop shape is $E = f_1(E\ddot{o})$. This model is justified by correlation 1, but the model is good for the low and the moderate viscosity ranges ($\mu_c < 4.0$ c.p.). The model $E = f_4(We)$ was found to more adequately represent droplet shape in all the viscosity

ranges (0.31 to 45.9 c.p.) than the model suggested by Harmathy. This conclusion is based on the analysis of correlation 4.

4. Deformation of a drop depends upon its size.

Larger drops of any system are found to be more deformed than smaller drops of the same system. The eccentricity of non-oscillating drops is directly proportional to the square of the equivalent drop diameters

$$E \propto d_e^2$$

and not to the first power of the equivalent drop diameter as suggested by previous authors.

5. Interfacial tension was found to be the most important of all the physical properties affecting the drop shape. Eccentricity was found to be almost inversely proportional to interfacial tension. The next important physical property of the system affecting the drop shape is $\Delta\rho$, the difference in densities of the continuous phase and dispersed phase liquids. Eccentricity is directly proportional to $\Delta\rho$. The continuous phase viscosity, μ_c , was found

to have a limited effect on shape. Its effect appears only in systems which have high viscosity ($\mu_c < 4.0$ c.p.). The least important of all physical properties affecting droplet shape is the dispersed phase viscosity, μ_d . The effect of both viscosities is to lessen the deformation of the drops, if all other physical properties are held constant.

VI. RECOMMENDATIONS

In this investigation only non-oscillating liquid droplets moving in liquid media were studied. The author's interest was limited to obtaining a correlation which could predict the eccentricity of non-oscillating drops. The following recommendations are made for further investigation of the topic:

1. Oscillating liquid drops are frequently encountered in practice. An attempt should be made to correlate the "time average" deformation of such drops. (a) The correlations developed in this study might be found good enough to also represent the mean eccentricity of oscillating drops. (b) $\ln(E \cdot R_e)$ versus $\ln(E_o \cdot W_e)$ plots were found to result in a set of parallel straight lines. A few data points representing oscillating drops were found by the author to fall exactly on these straight lines (points for oscillating drops are not shown in Figure 24). These parallel straight lines when brought together might represent a correlation for both oscillating and non-oscillating drops.

2. Drag coefficient, C , versus Reynolds number, Re , curves for liquid droplets moving in liquid media are reported in literature. The curves for droplets are markedly different from C versus Re curves of solid sphere. Because of the lack of eccentricity data for the droplets, C and Re were calculated assuming droplets to be perfect spheres. Now, with the eccentricity of drops known, it is possible to calculate their accurate frontal area. It is suggested that C versus Re curves should be reconstructed using the accurate frontal area in drag coefficient and a modified Reynolds number. The new curves would possibly be more accurate and would shed more light on the field of drop motion.
3. Because of the limited availability of funds, only two systems of high continuous phase viscosity could be studied in the present work. It is suggested that the investigation of the eccentricity of drops be extended to more systems which have high continuous phase viscosities.

VII. APPENDIX

Appendix A.Materials

Aniline: Technical grade aniline was distilled in an all glass apparatus.

Benzene: Technical grade benzene was distilled in an all glass apparatus.

Benzyl alcohol: Fischer Reagent quality benzyl alcohol.

Bromobenzene: Technical grade bromobenzene was distilled in an all glass apparatus.

Carbon tetrachloride: Technical grade CCl_4 was distilled in an all glass apparatus.

Corn oil: Mazola Corn Oil was used without distillation.

Ethylene glycol: Technical grade glycol was used without distillation.

Hexane: Technical grade and Fischer Reagent grade hexane was used without distillation.

Methyl isobutyl ketone: Technical grade MIBK was used without distillation.

Nitrobenzene: Fischer Reagent quality nitrobenzene.

Water: Distilled water from a laboratory still.

Appendix B.

TABLE IV

List of Liquid-Liquid Systems and their Sources

System No.	Dispersed Phase	Continuous Phase	Source
1.	Methyl ethyl ketone	Water	Klee & Treybal ⁽¹³⁾
2.	Sec-butyl alcohol	Water	"
3.	Water*	Furfural	"
4.	Nonyl alcohol	Water	"
5.	Water*	n-Heptylic acid	"
6.	Methyl isobutyl ketone	Water	"
7.	S.A.E. 10W oil	Water	"
8.	Benzene	Water	"
9.	Benzene	20% Sucrose solution	"
10.	Kerosene	Water	"
11.	Pentachloroethane	Water	"
12.	Glycol diacetate(pure)	Water	Wellek ⁽²⁴⁾
13.	Glycol diacetate (saturated)	Water	"
14.	Ethyl acetoacetate(pure)	Water	"
15.	Ethyl acetoacetate (saturated)	Water	"

* Not used in this work.

TABLE IV (continued)

System No.	Dispersed Phase	Continuous Phase	Source
16.	Glyceryl triacetate (pure)	Water	Wellek ⁽²⁴⁾
17.	Glyceryl triacetate (saturated)	Water	"
18.	2-Ethyl-hexane 1,3diol (saturated)	Water	Garner & Tayeban ⁽⁶⁾
19.	Benzyl alcohol (saturated)	Water	"
20.	n-Butyl alcohol	Water	Keith & Hixson ⁽¹¹⁾
21.	Ethyl acetate	Water	"
22.	Methyl isobutyl ketone	Water	"
23.	n-Butyl chloride	Water	"
24.	Toluene	Water	"
25.	Cyclohexane	Water	"
26.	Water	Benzyl alcohol	Skelland (22)
27.	Benzyl alcohol	Water	"
28.	Methyl isobutyl ketone	Water	"
29.	Water	Methyl isobutyl ketone	"
30.	Water	Benzaldehyde	"
31.	Benzaldehyde	Water	"
32.	Nitrobenzene	Water	"
33.	Water	Nitrobenzene	"

TABLE IV (continued)

System No.	Dispersed Phase	Continuous Phase	Source
34.	Water*	Benzene	Skelland (22)
35.	Benzene*	Water	"
36.	Water	Chlorobenzene	"
37.	Chlorobenzene	Water	"
38.	Ethylbenzene	Water	"
39.	Water	Ethylbenzene	"
40.	Nitrobenzene	Water	Present work
41.	Carbon tetrachloride	Water	"
42.	Water	Methyl isobutyl ketone	"
43.	Water	Hexane	"
44.	Bromobenzene	Water	"
45.	Aniline	Water	"
46.	Nitrobenzene	Glycol [#]	"
47.	Glycol [#]	Hexane	"
48.	Water	Corn oil	"
49.	Glycol [#]	Benzene	"

* Not used in this work.

Ethylene glycol

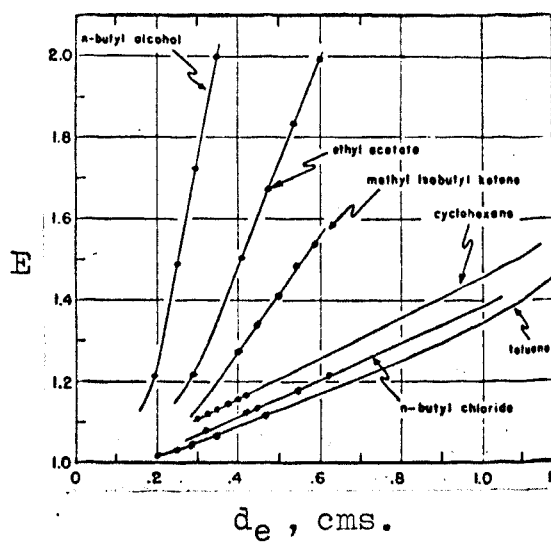


Figure 23. Keith and Hixson (//) eccentricity data investigated in this work.

TABLE V

Physical Properties, Equivalent Diameter, Velocity and
Eccentricity of Droplets

No. n*s	σ_i dynes/cm	ρ_c gm/ml	ρ_d gm/ml	μ_c c.p.	μ_d c.p.	d_e cm	U_t cm/sec	E
1* 1	.30	.9600	.8370	1.45	.60	.040	2.00	1.00
2* 1	.30	.9600	.8370	1.45	.60	.060	2.60	1.00
3* 1	.30	.9600	.8370	1.45	.60	.060	2.60	1.18
4* 1	.30	.9600	.8370	1.45	.60	.070	3.10	1.46
5* 1	.30	.9600	.8370	1.45	.60	.120	4.40	2.14
6* 1	.30	.9600	.8370	1.45	.60	.130	4.70	1.72
7* 1	.30	.9600	.8370	1.45	.60	.150	5.00	2.11
1* 2	.60	.9705	.8660	1.56	2.78	.080	2.90	1.13
2* 2	.60	.9705	.8660	1.56	2.78	.090	3.20	1.18
3* 2	.60	.9705	.8660	1.56	2.78	.110	3.60	1.26
4* 2	.60	.9705	.8660	1.56	2.78	.150	4.40	1.27
5* 2	.60	.9705	.8660	1.56	2.78	.160	4.60	1.48
6* 2	.60	.9705	.8660	1.56	2.78	.210	5.30	1.88
7* 2	.60	.9705	.8660	1.56	2.78	.220	5.40	2.08
8* 2	.60	.9705	.8660	1.56	2.78	.230	5.50	2.34
1* 4	4.90	.9982	.8242	1.00	16.20	.190	5.51	1.18
2* 4	4.90	.9982	.8242	1.00	16.20	.220	7.60	1.23
3* 4	4.90	.9982	.8242	1.00	16.20	.240	8.00	1.21
4* 4	4.90	.9982	.8242	1.00	16.20	.290	8.75	1.24
5* 4	4.90	.9982	.8242	1.00	16.20	.410	9.50	1.69
1* 6	9.80	.9947	.8155	.93	.60	.090	4.30	1.00
2* 6	9.80	.9947	.8155	.93	.60	.120	5.40	1.04
3* 6	9.80	.9947	.8155	.93	.60	.140	5.50	1.08
4* 6	9.80	.9947	.8155	.93	.60	.150	5.80	1.00
5* 6	9.80	.9947	.8155	.93	.60	.160	6.30	1.10
6* 6	9.80	.9947	.8155	.93	.60	.210	7.60	1.13
7* 6	9.80	.9947	.8155	.93	.60	.230	8.60	1.09
8* 6	9.80	.9947	.8155	.93	.60	.240	8.70	1.13
9* 6	9.80	.9947	.8155	.93	.60	.280	9.80	1.15
10* 6	9.80	.9947	.8155	.93	.60	.320	10.40	1.21
1* 7	18.50	.9975	.8650	1.06	72.10	.200	6.30	1.05
2* 7	18.50	.9975	.8650	1.06	72.10	.230	7.00	1.07
3* 7	18.50	.9975	.8650	1.06	72.10	.300	7.90	1.12
4* 7	18.50	.9975	.8650	1.06	72.10	.350	9.40	1.12
5* 7	18.50	.9975	.8650	1.06	72.10	.390	10.10	1.16
6* 7	18.50	.9975	.8650	1.06	72.10	.450	10.80	1.19
7* 7	18.50	.9975	.8650	1.06	72.10	.530	11.20	1.27
8* 7	18.50	.9975	.8650	1.06	72.10	.590	11.80	1.22
9* 7	18.50	.9975	.8650	1.06	72.10	.690	11.00	1.40
10* 7	18.50	.9975	.8650	1.06	72.10	.720	11.00	1.36
11* 7	18.50	.9975	.8650	1.06	72.10	.900	10.80	1.46
12* 7	18.50	.9975	.8650	1.06	72.10	1.200	10.80	1.73
1* 8	30.00	.9975	.8870	1.14	.68	.200	5.40	1.07
2* 8	30.00	.9975	.8870	1.14	.68	.220	5.85	1.05
3* 8	30.00	.9975	.8870	1.14	.68	.280	7.05	1.10
4* 8	30.00	.9975	.8870	1.14	.68	.370	8.50	1.08
5* 8	30.00	.9975	.8870	1.14	.68	.460	9.10	1.15
6* 8	30.00	.9975	.8870	1.14	.68	.600	10.80	1.24
7* 8	30.00	.9975	.8870	1.14	.68	.670	11.45	1.20
8* 8	30.00	.9975	.8870	1.14	.68	.770	11.70	1.32
1* 9	30.10	1.0600	.8720	1.39	.59	.290	9.00	1.07
2* 9	30.10	1.0600	.8720	1.39	.59	.350	10.70	1.12
3* 9	30.10	1.0600	.8720	1.39	.59	.450	12.10	1.15
4* 9	30.10	1.0600	.8720	1.39	.59	.530	13.40	1.20
5* 9	30.10	1.0600	.8720	1.39	.59	.620	13.70	1.26
1* 10	40.40	.9986	.8071	1.08	1.47	.230	8.30	1.07
2* 10	40.40	.9986	.8071	1.08	1.47	.330	10.65	1.09
3* 10	40.40	.9986	.8071	1.08	1.47	.430	12.50	1.15
4* 10	40.40	.9986	.8071	1.08	1.47	.490	13.50	1.18
5* 10	40.40	.9986	.8071	1.08	1.47	.510	13.90	1.15
6* 10	40.40	.9986	.8071	1.08	1.47	.580	13.90	1.21
7* 10	40.40	.9986	.8071	1.08	1.47	.630	14.70	1.20
1* 11	42.40	.9978	1.6740	.95	2.03	.170	14.00	1.07
2* 11	42.40	.9978	1.6740	.95	2.03	.240	17.40	1.12
3* 11	42.40	.9978	1.6740	.95	2.03	.290	19.50	1.14

TABLE V (continued)

No. n*s	σ_i dynes/cm	ρ_c gm/ml	ρ_d gm/ml	μ_c c.p.	μ_d c.p.	d_e cm	U_c cm/sec	E
4*11	42.40	.9978	1.6740	.95	2.03	.330	20.30	1.15
5*11	42.40	.9978	1.6740	.95	2.03	.380	20.20	1.24
1*12	2.33	.9971	1.0990	.92	2.62	.144	2.79	1.03
2*12	2.33	.9971	1.0990	.92	2.62	.224	4.58	1.25
3*12	2.33	.9971	1.0990	.92	2.62	.243	4.78	1.44
4*12	2.33	.9971	1.0990	.92	2.62	.280	6.16	1.61
1*13	2.33	.9971	1.0976	.92	2.44	.144	2.88	1.02
2*13	2.33	.9971	1.0976	.92	2.44	.226	4.84	1.30
3*13	2.33	.9971	1.0976	.92	2.44	.249	5.27	1.44
4*13	2.33	.9971	1.0976	.92	2.44	.268	5.45	1.61
1*14	3.50	.9970	1.0194	.90	1.50	.305	2.11	1.02
2*14	3.50	.9970	1.0194	.90	1.50	.456	3.77	1.15
3*14	3.50	.9970	1.0194	.90	1.50	.559	4.28	1.36
1*15	3.50	.9970	1.0220	.90	1.58	.299	2.43	1.01
2*15	3.50	.9970	1.0220	.90	1.58	.418	3.67	1.12
3*15	3.50	.9970	1.0220	.90	1.58	.518	4.56	1.38
1*16	3.99	.9971	1.1531	.91	16.60	.151	5.43	1.05
2*16	3.99	.9971	1.1531	.91	16.60	.206	7.01	1.18
3*16	3.99	.9971	1.1531	.91	16.60	.263	8.30	1.34
4*16	3.99	.9971	1.1531	.91	16.60	.260	8.30	1.34
1*17	3.99	.9971	1.1472	.91	10.90	.177	4.61	1.07
2*17	3.99	.9971	1.1472	.91	10.90	.233	7.75	1.24
3*17	3.99	.9971	1.1472	.91	10.90	.268	8.52	1.37
4*17	3.99	.9971	1.1472	.91	10.90	.267	8.48	1.35
1*18	4.00	.9982	.9450	1.00	85.00	.185	2.38	1.00
2*18	4.00	.9982	.9450	1.00	85.00	.210	3.34	1.00
3*18	4.00	.9982	.9450	1.00	85.00	.245	3.88	1.05
4*18	4.00	.9982	.9450	1.00	85.00	.340	5.60	1.15
5*18	4.00	.9982	.9450	1.00	85.00	.355	5.93	1.20
1*19	5.00	.9982	1.0420	1.00	5.30	.230	3.92	1.01
2*19	5.00	.9982	1.0420	1.00	5.30	.295	6.11	1.03
3*19	5.00	.9982	1.0420	1.00	5.30	.330	5.77	1.09
4*19	5.00	.9982	1.0420	1.00	5.30	.350	6.01	1.12
5*19	5.00	.9982	1.0420	1.00	5.30	.408	6.88	1.30
6*19	5.00	.9982	1.0420	1.00	5.30	.425	7.31	1.32
1*20	1.80	.9865	.8427	1.19	2.74	.200	7.90	1.21
2*20	1.80	.9865	.8427	1.19	2.74	.250	7.97	1.48
3*20	1.80	.9865	.8427	1.19	2.74	.300	8.04	1.72
4*20	1.80	.9865	.8427	1.19	2.74	.350	8.10	2.00
1*21	4.50	.9922	.8988	1.20	.48	.288	7.25	1.21
2*21	4.50	.9922	.8988	1.20	.48	.413	7.30	1.50
3*21	4.50	.9922	.8988	1.20	.48	.475	7.38	1.66
4*21	4.50	.9922	.8988	1.20	.48	.537	7.50	1.82
5*21	4.50	.9922	.8988	1.20	.48	.600	7.56	1.99
1*22	10.70	.9950	.8006	.93	.58	.400	10.75	1.27
2*22	10.70	.9950	.8006	.93	.58	.450	10.75	1.33
3*22	10.70	.9950	.8006	.93	.58	.500	10.75	1.41
4*22	10.70	.9950	.8006	.93	.58	.550	10.75	1.48
5*22	10.70	.9950	.8006	.93	.58	.590	10.75	1.54
1*23	24.20	.9957	.8784	.92	.43	.325	8.00	1.08
2*23	24.20	.9957	.8784	.92	.43	.413	9.75	1.12
3*23	24.20	.9957	.8784	.92	.43	.450	10.25	1.14
4*23	24.20	.9957	.8784	.92	.43	.544	11.00	1.18
5*23	24.20	.9957	.8784	.92	.43	.613	11.00	1.21
1*24	35.60	.9969	.8606	.89	.55	.200	7.25	1.02
2*24	35.60	.9969	.8606	.89	.55	.225	8.05	1.03
3*24	35.60	.9969	.8606	.89	.55	.288	9.50	1.05
4*24	35.60	.9969	.8606	.89	.55	.350	10.45	1.07
5*24	35.60	.9969	.8606	.89	.55	.467	11.25	1.11
1*25	40.70	.9968	.7723	.90	.88	.300	13.25	1.10
2*25	40.70	.9968	.7723	.90	.88	.325	13.50	1.12
3*25	40.70	.9968	.7723	.90	.88	.350	13.73	1.13
4*25	40.70	.9968	.7723	.90	.88	.375	13.85	1.14
5*25	40.70	.9968	.7723	.90	.88	.400	13.98	1.15
6*25	40.70	.9968	.7723	.90	.88	.413	14.00	1.16
1*26	3.60	1.0394	.9964	4.09	.85	.257	2.52	1.04
2*26	3.60	1.0394	.9964	4.09	.85	.280	2.61	1.05
3*26	3.60	1.0395	.9964	4.70	.85	.289	2.89	1.07
4*26	3.60	1.0396	.9965	4.72	.85	.327	3.37	1.11
5*26	3.60	1.0397	.9965	4.73	.85	.368	3.96	1.13
6*26	3.60	1.0398	.9965	4.76	.85	.438	4.77	1.24

TABLE V (continued)

No. n*s	σ_i dynes/cm	ρ_c gm/ml	ρ_a gm/ml	μ_c c.p.	μ_a c.p.	d_c cm	U_c cm/sec	E
1*27	3.60	.9965	1.0398	.85	4.76	.287	4.19	1.12
2*27	3.60	.9965	1.0397	.85	4.73	.322	4.81	1.13
3*27	3.60	.9965	1.0396	.85	4.72	.344	4.92	1.14
4*27	3.60	.9965	1.0396	.85	4.72	.380	5.54	1.24
5*27	3.60	.9964	1.0394	.85	4.69	.421	6.02	1.34
6*27	3.60	.9964	1.0394	.85	4.69	.470	6.73	1.53
1*28	10.20	.9969	.8011	.89	.58	.204	9.66	1.19
2*28	10.20	.9969	.8011	.89	.58	.210	12.13	1.32
1*29	10.40	.7956	.9958	.54	.81	.236	14.47	1.58
2*29	10.40	.7956	.9958	.54	.81	.245	14.59	1.55
1*30	14.20	1.0368	.9961	1.30	.82	.371	7.42	1.11
2*30	14.15	1.0365	.9960	1.29	.82	.418	8.41	1.23
3*30	14.15	1.0365	.9960	1.29	.82	.462	9.72	1.41
4*30	14.15	1.0365	.9960	1.29	.82	.508	9.84	1.43
5*30	14.15	1.0365	.9960	1.29	.82	.583	9.89	1.71
1*31	14.40	.9965	1.0380	.85	1.33	.379	7.72	1.10
2*31	14.45	.9965	1.0383	.85	1.33	.414	8.68	1.24
3*31	14.30	.9963	1.0374	.84	1.31	.438	9.64	1.31
4*31	14.30	.9963	1.0375	.84	1.31	.501	9.84	1.11
5*31	14.30	.9963	1.0374	.84	1.31	.538	9.95	1.50
1*32	22.10	.9968	1.1974	.88	1.78	.301	16.67	1.29
2*32	22.20	.9969	1.1975	.88	1.79	.314	16.97	1.32
1*33	22.20	1.1975	.9969	1.78	.88	.273	9.92	1.10
2*33	22.20	1.1975	.9969	1.78	.88	.294	9.92	1.09
3*33	23.80	1.1995	.9974	1.84	.92	.314	10.17	1.09
1*36	33.50	1.0950	.9955	.71	.79	.402	10.14	1.08
2*36	34.20	1.0965	.9959	.72	.81	.449	10.52	1.11
3*36	33.80	1.0955	.9956	.72	.80	.502	10.75	1.12
1*37	35.00	.9965	1.0988	.85	.74	.380	9.84	1.17
2*37	35.00	.9965	1.0988	.85	.74	.452	12.03	1.20
3*37	35.00	.9965	1.0988	.85	.74	.465	12.39	1.50
4*37	35.00	.9966	1.0990	.87	.74	.521	12.80	1.63
5*37	35.00	.9966	1.0990	.87	.74	.577	13.46	1.69
1*38	34.80	.9964	.8601	.85	.62	.337	9.91	1.06
2*38	34.80	.9965	.8602	.85	.62	.371	10.83	1.11
3*38	34.70	.9965	.8604	.85	.62	.421	12.08	1.15
4*38	34.70	.9965	.8603	.85	.62	.500	13.83	1.20
1*39	34.15	.8619	.9970	.63	.89	.405	14.28	1.55
2*39	34.15	.8618	.9969	.63	.90	.433	14.63	1.62
3*39	35.25	.8591	.9962	.61	.83	.465	14.92	1.70
4*39	35.25	.8591	.9962	.61	.83	.505	15.29	1.76
5*39	35.25	.8591	.9962	.61	.83	.589	15.77	1.80
1*40	13.50	.9973	1.1963	.85	1.71	.284	16.02	1.32
2*40	13.50	.9973	1.1963	.85	1.71	.301	16.41	1.52
1*41	31.10	.9964	1.5782	.85	.89	.223	22.26	1.13
1*42	9.74	.7985	.9941	.55	.87	.230	14.58	1.54
2*42	9.74	.7985	.9941	.55	.87	.234	14.55	1.65
1*43	32.10	.6655	.9961	.32	.84	.325	20.04	1.11
1*44	34.20	.9967	1.0985	.83	.73	.437	11.09	1.12
1*45	6.60	.9973	1.0157	.86	3.08	.437	3.94	1.09
2*45	6.60	.9973	1.0157	.86	3.08	.503	4.63	1.16
3*45	6.60	.9973	1.0157	.86	3.08	.531	4.95	1.21
4*45	6.60	.9973	1.0157	.86	3.08	.612	5.57	1.41
5*45	6.60	.9973	1.0157	.86	3.08	.665	5.87	1.61
1*46	4.88	1.1134	1.1952	13.55	1.78	.352	3.39	1.11
2*46	4.88	1.1134	1.1952	13.55	1.78	.376	3.69	1.11
3*46	4.88	1.1134	1.1952	13.55	1.78	.414	4.11	1.16
4*46	4.88	1.1134	1.1952	13.55	1.78	.437	4.33	1.23
5*46	4.88	1.1134	1.1952	13.55	1.78	.481	4.79	1.31
1*47	14.20	.6657	1.1057	.31	14.56	.193	17.16	1.14
2*47	14.20	.6657	1.1057	.31	14.56	.218	18.02	1.17
3*47	14.20	.6657	1.1057	.31	14.56	.244	18.79	1.23
4*47	14.20	.6657	1.1057	.31	14.56	.254	19.13	1.23
5*47	14.20	.6657	1.1057	.31	14.56	.285	19.81	1.41
1*48	23.40	.9135	.9997	45.93	.86	.795	3.80	1.06
2*48	23.40	.9135	.9997	45.93	.86	.951	4.61	1.12
3*48	23.40	.9135	.9997	45.93	.86	1.016	5.08	1.14
1*49	7.38	.8689	1.0936	.57	12.21	.190	9.31	1.22
2*49	7.38	.8689	1.0936	.57	12.21	.218	10.13	1.23
3*49	7.38	.8689	1.0936	.57	12.21	.236	10.54	1.31
4*49	7.38	.8689	1.0936	.57	12.21	.264	11.13	1.38
5*49	7.38	.8689	1.0936	.57	12.21	.279	11.36	1.47

Dimensionless Groups

No. n*s	μ_c/μ_b	Re	We	Eo	Fr	C	P
1* 1	2.416	5.29	.51	.64	.10	1.67	4669.851E+00
2* 1	2.416	10.32	1.29	1.44	.11	1.48	4669.851E+00
3* 1	2.416	10.32	1.29	1.44	.11	1.48	4669.851E+00
4* 1	2.416	14.36	2.15	1.96	.14	1.21	4669.851E+00
5* 1	2.416	34.95	7.43	5.78	.16	1.03	4669.851E+00
6* 1	2.416	40.45	9.18	6.79	.17	.98	4669.851E+00
7* 1	2.416	49.65	12.00	9.04	.17	1.00	4669.851E+00
1* 2	.561	14.43	1.08	1.09	.10	1.33	3354.316E+01
2* 2	.561	17.91	1.49	1.38	.11	1.23	3354.316E+01
3* 2	.561	24.63	2.30	2.06	.12	1.19	3354.316E+01
4* 2	.561	41.05	4.69	3.84	.13	1.09	3354.316E+01
5* 2	.561	45.78	5.47	4.36	.13	1.06	3354.316E+01
6* 2	.561	69.24	9.54	7.52	.13	1.05	3354.316E+01
7* 2	.561	73.90	10.37	8.26	.13	1.06	3354.316E+01
8* 2	.561	78.69	11.25	9.02	.13	1.06	3354.316E+01
1* 4	.061	104.50	1.17	1.25	.16	1.42	6874.609E+04
2* 4	.061	166.89	2.58	1.68	.26	.86	6874.609E+04
3* 4	.061	191.65	3.12	2.00	.27	.85	6874.609E+04
4* 4	.061	253.29	4.52	2.92	.26	.86	6874.609E+04
5* 4	.061	388.79	7.53	5.84	.22	1.03	6874.609E+04
1* 6	1.550	41.39	.16	.14	.20	1.14	7088.699E+05
2* 6	1.550	69.30	.35	.25	.24	.96	7088.699E+05
3* 6	1.550	82.35	.42	.35	.22	1.08	7088.699E+05
4* 6	1.550	93.05	.51	.40	.22	1.04	7088.699E+05
5* 6	1.550	107.81	.64	.45	.25	.94	7088.699E+05
6* 6	1.550	170.70	1.23	.79	.28	.85	7088.699E+05
7* 6	1.550	211.56	1.72	.94	.32	.73	7088.699E+05
8* 6	1.550	223.32	1.84	1.03	.32	.74	7088.699E+05
9* 6	1.550	293.48	2.72	1.40	.35	.68	7088.699E+05
10* 6	1.550	355.95	3.51	1.83	.34	.69	7088.699E+05
1* 7	.014	118.57	.42	.28	.20	.87	3843.046E+06
2* 7	.014	151.50	.60	.37	.21	.81	3843.046E+06
3* 7	.014	223.02	1.00	.63	.21	.83	3843.046E+06
4* 7	.014	309.60	1.66	.85	.25	.68	3843.046E+06
5* 7	.014	370.67	2.14	1.06	.26	.66	3843.046E+06
6* 7	.014	457.34	2.83	1.42	.26	.66	3843.046E+06
7* 7	.014	558.60	3.58	1.97	.24	.73	3843.046E+06
8* 7	.014	655.15	4.42	2.44	.24	.73	3843.046E+06
9* 7	.014	714.24	4.50	3.34	.17	.98	3843.046E+06
10* 7	.014	745.30	4.69	3.63	.17	1.03	3843.046E+06
11* 7	.014	914.68	5.66	5.68	.13	1.33	3843.046E+06
12* 7	.014	1219.58	7.54	10.10	.09	1.78	3843.046E+06
1* 8	1.676	94.50	.19	.14	.14	.99	1468.864E+07
2* 8	1.676	112.61	.25	.17	.15	.93	1468.864E+07
3* 8	1.676	172.72	.46	.28	.18	.81	1468.864E+07
4* 8	1.676	275.18	.88	.49	.19	.74	1468.864E+07
5* 8	1.676	366.27	1.26	.76	.18	.80	1468.864E+07
6* 8	1.676	567.00	2.32	1.29	.19	.74	1468.864E+07
7* 8	1.676	671.25	2.92	1.62	.19	.73	1468.864E+07
8* 8	1.676	788.28	3.50	2.14	.18	.81	1468.864E+07
1* 9	2.355	199.03	.82	.51	.28	.82	4455.209E+06
2* 9	2.355	285.58	1.41	.74	.33	.70	4455.209E+06
3* 9	2.355	415.23	2.32	1.23	.33	.71	4455.209E+06
4* 9	2.355	541.59	3.35	1.71	.34	.68	4455.209E+06
5* 9	2.355	647.74	4.09	2.35	.30	.76	4455.209E+06
1*10	.734	176.51	.39	.24	.30	.83	2575.356E+07
2*10	.734	324.96	.92	.50	.35	.72	2575.356E+07
3*10	.734	496.98	1.66	.85	.37	.68	2575.356E+07
4*10	.734	611.64	2.20	1.11	.37	.67	2575.356E+07
5*10	.734	655.46	2.43	1.20	.38	.66	2575.356E+07
6*10	.734	745.43	2.76	1.56	.33	.75	2575.356E+07
7*10	.734	856.29	3.36	1.84	.35	.73	2575.356E+07
1*11	.467	249.97	.78	.45	1.17	.76	1406.011E+07
2*11	.467	438.61	1.70	.90	1.28	.70	1406.011E+07
3*11	.467	593.95	2.59	1.31	1.33	.67	1406.011E+07
4*11	.467	703.60	3.20	1.70	1.27	.70	1406.011E+07
5*11	.467	806.22	3.64	2.25	1.09	.82	1406.011E+07

TABLE VI (continued)

No. n*s	μ_c/μ_0	Re	We	Eu	Fr	C	P
1*12	.351	43.54	.47	.88	.05	2.47	1757.897E+04
2*12	.351	111.18	2.01	2.15	.09	1.42	1757.897E+04
3*12	.351	125.88	2.37	2.53	.09	1.42	1757.897E+04
4*12	.351	186.93	4.54	3.36	.13	.98	1757.897E+04
1*13	.377	44.94	.51	.87	.05	2.28	1782.385E+04
2*13	.377	118.55	2.26	2.15	.10	1.27	1782.385E+04
3*13	.377	142.22	2.95	2.62	.11	1.18	1782.385E+04
4*13	.377	158.30	3.40	3.03	.11	1.18	1782.385E+04
1*14	.600	71.29	.38	.58	.01	2.01	2959.036E+05
2*14	.600	190.44	1.84	1.30	.03	.94	2959.036E+05
3*14	.600	265.03	2.91	1.95	.03	.89	2959.036E+05
1*15	.569	80.48	.50	.62	.02	1.65	2651.296E+05
2*15	.569	169.93	1.60	1.22	.03	1.01	2651.296E+05
3*15	.569	261.66	3.06	1.87	.04	.81	2651.296E+05
1*16	.054	89.84	1.11	.87	.19	1.04	6023.929E+04
2*16	.054	158.22	2.52	1.62	.24	.85	6023.929E+04
3*16	.054	239.18	4.52	2.65	.26	.78	6023.929E+04
4*16	.054	236.45	4.47	2.59	.27	.77	6023.929E+04
1*17	.083	89.40	.94	1.15	.12	1.63	6260.713E+04
2*17	.083	197.85	3.49	2.00	.26	.76	6260.713E+04
3*17	.083	250.19	4.86	2.64	.27	.72	6260.713E+04
4*17	.083	248.08	4.79	2.62	.27	.73	6260.713E+04
1*18	.011	43.95	.26	.44	.03	2.27	1223.143E+05
2*18	.011	70.01	.58	.57	.05	1.31	1223.143E+05
3*18	.011	94.88	.92	.78	.06	1.13	1223.143E+05
4*18	.011	190.05	2.66	1.50	.09	.75	1223.143E+05
5*18	.011	210.13	3.11	1.64	.10	.70	1223.143E+05
1*19	.188	89.99	.70	.45	.06	.85	2901.649E+05
2*19	.188	179.92	2.19	.74	.12	.45	2901.649E+05
3*19	.188	190.06	2.19	.93	.10	.56	2901.649E+05
4*19	.188	209.97	2.52	1.05	.10	.55	2901.649E+05
5*19	.188	280.19	3.85	1.42	.11	.49	2901.649E+05
6*19	.188	310.11	4.53	1.55	.12	.45	2901.649E+05
1*20	.434	130.98	6.84	3.13	.31	.61	2008.347E+03
2*20	.434	165.17	8.70	4.89	.25	.74	2008.347E+03
3*20	.434	199.95	10.62	7.04	.21	.88	2008.347E+03
4*20	.434	235.01	12.58	9.59	.19	1.01	2008.347E+03
1*21	2.500	172.64	3.33	1.68	.18	.67	4726.482E+04
2*21	2.500	249.28	4.85	3.46	.13	.95	4726.482E+04
3*21	2.500	289.84	5.70	4.58	.11	1.07	4726.482E+04
4*21	2.500	333.00	6.66	5.86	.10	1.17	4726.482E+04
5*21	2.500	375.05	7.56	7.32	.09	1.29	4726.482E+04
1*22	1.603	460.05	4.29	2.84	.29	.88	8510.270E+05
2*22	1.603	517.56	4.83	3.60	.26	.99	8510.270E+05
3*22	1.603	575.06	5.37	4.45	.23	1.10	8510.270E+05
4*22	1.603	632.57	5.91	5.38	.21	1.21	8510.270E+05
5*22	1.603	678.57	6.34	6.19	.19	1.30	8510.270E+05
1*23	2.139	281.39	.85	.50	.20	.78	1706.191E+07
2*23	2.139	435.80	1.61	.81	.23	.66	1706.191E+07
3*23	2.139	499.20	1.94	.96	.23	.65	1706.191E+07
4*23	2.139	647.63	2.70	1.40	.22	.69	1706.191E+07
5*23	2.139	729.78	3.05	1.78	.20	.77	1706.191E+07
1*24	1.618	162.41	.29	.15	.26	.67	5350.214E+07
2*24	1.618	202.88	.40	.18	.29	.62	5350.214E+07
3*24	1.618	306.46	.72	.31	.31	.57	5350.214E+07
4*24	1.618	409.68	1.07	.45	.31	.57	5350.214E+07
5*24	1.618	588.47	1.65	.81	.27	.65	5350.214E+07
1*25	1.022	440.25	1.28	.48	.59	.50	4640.735E+07
2*25	1.022	485.94	1.45	.57	.57	.52	4640.735E+07
3*25	1.022	532.23	1.61	.66	.54	.54	4640.735E+07
4*25	1.022	575.23	1.76	.76	.52	.57	4640.735E+07
5*25	1.022	619.34	1.91	.86	.49	.60	4640.735E+07
6*25	1.022	640.38	1.98	.92	.48	.62	4640.735E+07
1*26	5.517	14.35	.47	.77	.02	2.18	2472.219E+02
2*26	5.517	17.43	.63	.91	.02	1.91	2472.219E+02
3*26	5.529	18.47	.69	.97	.02	1.87	2446.029E+02
4*26	5.552	24.27	1.07	1.25	.03	1.55	2405.296E+02
5*26	5.564	32.03	1.66	1.59	.04	1.27	2379.957E+02
6*26	5.600	45.63	2.87	2.26	.05	1.04	2315.609E+02
1*27	.178	140.97	1.39	.97	.06	.92	2091.570E+05

TABLE VI (continued)

No. n*s	μ_c/μ_b	Re	We	Eo	Fr	C	P
2*27	.179	181.57	2.06	1.21	.07	.78	2096.411E+05
3*27	.180	198.41	2.30	1.38	.07	.80	2101.275E+05
4*27	.180	246.80	3.22	1.69	.08	.69	2101.275E+05
5*27	.181	297.09	4.22	2.07	.08	.65	2105.739E+05
6*27	.181	370.78	5.89	2.58	.09	.58	2105.739E+05
1*28	1.534	220.73	1.86	.78	.46	.56	8760.016E+05
2*28	1.534	285.32	3.01	.82	.71	.36	8760.016E+05
1*29	.666	503.13	3.78	1.05	.90	.37	4267.999E+06
2*29	.666	526.65	3.98	1.13	.88	.37	4267.999E+06
1*30	1.585	219.54	1.49	.38	.15	.34	2701.849E+06
2*30	1.573	282.45	2.16	.49	.17	.30	2769.286E+06
3*30	1.573	360.81	3.19	.59	.20	.24	2769.286E+06
4*30	1.573	401.64	3.60	.72	.19	.26	2769.286E+06
5*30	1.573	463.28	4.17	.95	.17	.30	2769.286E+06
1*31	.639	343.01	1.56	.40	.16	.34	1396.664E+07
2*31	.639	421.28	2.15	.48	.18	.30	1401.135E+07
3*31	.641	500.79	2.83	.54	.21	.25	1447.449E+07
4*31	.641	584.71	3.37	.70	.19	.27	1443.935E+07
5*31	.641	634.91	3.71	.81	.18	.29	1447.449E+07
1*32	.494	568.36	3.77	.80	.94	.28	9097.145E+06
2*32	.491	603.64	4.06	.87	.93	.28	9223.046E+06
1*33	2.022	182.19	1.44	.65	.36	.60	7950.106E+05
2*33	2.022	196.20	1.56	.76	.34	.65	7950.106E+05
3*33	2.000	208.17	1.63	.82	.33	.66	8544.126E+05
1*36	.898	628.66	1.35	.47	.26	.46	1819.198E+08
2*36	.888	719.34	1.59	.58	.25	.48	1815.271E+08
3*36	.900	821.09	1.88	.72	.23	.51	1761.380E+08
1*37	1.148	438.36	1.04	.41	.26	.52	8135.445E+07
2*37	1.148	637.47	1.86	.58	.32	.41	8135.445E+07
3*37	1.148	675.43	2.03	.61	.33	.40	8135.445E+07
4*37	1.175	763.92	2.43	.77	.32	.42	7407.008E+07
5*37	1.175	889.65	2.97	.95	.32	.42	7407.008E+07
1*38	1.370	391.48	.94	.43	.29	.61	6000.777E+07
2*38	1.370	471.04	1.24	.52	.32	.56	6001.982E+07
3*38	1.370	596.22	1.76	.68	.35	.51	5959.133E+07
4*38	1.370	810.68	2.74	.96	.39	.46	5954.758E+07
1*39	.707	791.22	2.08	.63	.51	.40	1418.542E+08
2*39	.700	866.55	2.33	.72	.50	.41	1418.213E+08
3*39	.734	977.09	2.52	.82	.48	.43	1737.728E+08
4*39	.734	1087.45	2.87	.97	.47	.45	1737.728E+08
5*39	.734	1308.16	3.56	1.32	.43	.49	1737.728E+08
1*40	.497	533.81	5.38	1.16	.92	.28	2403.798E+06
2*40	.497	579.53	5.98	1.30	.91	.29	2403.798E+06
1*41	.955	581.89	3.54	.91	2.26	.34	1003.397E+07
1*42	.632	486.85	4.00	1.04	.94	.34	3358.775E+06
2*42	.632	494.30	4.06	1.07	.92	.35	3358.775E+06
1*43	.380	1354.50	2.70	1.06	1.26	.52	4312.035E+08
1*44	1.136	581.96	1.56	.55	.28	.47	8393.073E+07
1*45	.279	199.66	1.02	.52	.03	.67	2898.983E+06
2*45	.279	270.06	1.62	.69	.04	.56	2898.983E+06
3*45	.279	304.80	1.96	.77	.04	.52	2898.983E+06
4*45	.279	395.30	2.86	1.02	.05	.47	2898.983E+06
5*45	.279	452.67	3.46	1.20	.05	.46	2898.983E+06
1*46	7.612	9.80	.92	2.03	.03	2.94	5331.204E+00
2*46	7.612	11.40	1.16	2.32	.03	2.65	5331.204E+00
3*46	7.612	13.98	1.59	2.81	.04	2.35	5331.204E+00
4*46	7.612	15.54	1.86	3.13	.04	2.23	5331.204E+00
5*46	7.612	18.93	2.51	3.80	.04	2.01	5331.204E+00
1*47	.021	711.19	2.66	1.13	1.55	.56	3186.372E+07
2*47	.021	843.58	3.31	1.44	1.51	.57	3186.372E+07
3*47	.021	984.54	4.03	1.80	1.47	.59	3186.372E+07
4*47	.021	1043.43	4.35	1.95	1.47	.59	3186.372E+07
5*47	.021	1212.40	5.24	2.46	1.40	.62	3186.372E+07
1*48	53.406	6.00	.44	2.28	.01	6.78	2844.104E+00
2*48	53.406	8.71	.78	3.26	.02	5.51	2844.104E+00
3*48	53.406	10.26	1.02	3.72	.02	4.85	2844.104E+00
1*49	.046	269.64	1.93	1.07	.46	.74	1305.509E+06
2*49	.046	336.63	2.63	1.41	.48	.71	1305.509E+06
3*49	.046	379.18	3.08	1.66	.48	.71	1305.509E+06
4*49	.046	447.91	3.85	2.07	.47	.72	1305.509E+06
5*49	.046	483.14	4.23	2.32	.47	.73	1305.509E+06

Appendix C.

Results

Fortran Computer Program for Calculation of Eccentricity by Correlations

One through Six

```
C  COMPARISON OF THE CORRELATIONS
-----
DIMENSION EC(10),ER(10),TER(10),AER(10)
PUNCH 10
DO 5 I=1,6
-----
5  TER(I)=0.0
   DO 7 K=1,208
   READ 100,J,N,ST,DC,DD,VC,VD,DE,VT,E
   AD=ABSF(DC-DD)
   VV=VC/VD
   EO=980.*AD*DE**2/ST
   WE=DC*DE*VT**2/ST
   EC(1)=1.+.123*EO
   EC(2)=0.8153+0.2199*EO-0.005288*EO**2+0.00004472*EO**3
   EC(3)=66.089*AD**2*.79*DE**1.916*ST**(-.823)*VC**(-.441)*VD**(-.114)
   EC(3)=1.+EC(3)
   EC(4)=1.+.090992*WE**2*.953
   EC(5)=1.+.092274*WE**2*.984*VV**2*.063
   EC(6)=1.+.13683*VT**2*1.812*DE**1.072*ST**(-.971)*VD**(-.078)
   PRINT 200,J,N,DE,E,EC(1),EC(2),EC(3),EC(4),EC(5),EC(6)
   DO 7 I=1,6
   ER(I)=ABSF(E-EC(I))*100./E
7  TER(I)=TER(I)+ER(I)
-----
PUNCH 10
DO 9 I=1,6
AER(I)=TER(I)/208.
-----
9  PRINT 300,I,AER(I)
10 FORMAT(////)
100 FORMAT (I3,I5,8F8.4)
-----
200 FORMAT (I3,1H*,I2,F7.3,7F7.2)
300 FORMAT(45H AVERAGE PERCENTAGE DEVIATION FOR CORRELATION,I2,F8.2)
CALL EXIT
END
```

TABLE VII

Observed Eccentricity and Calculated Eccentricities

Calculated by Correlations 1 through 6

No. n*s	d _e	E _{obs}	E ₁	E ₂	E ₃	E ₄	E ₅	E ₆
1* 1	.040	1.00	1.07	.95	1.06	1.04	1.05	1.05
2* 1	.060	1.00	1.17	1.12	1.13	1.11	1.12	1.12
3* 1	.060	1.18	1.17	1.12	1.13	1.11	1.12	1.12
4* 1	.070	1.46	1.24	1.22	1.18	1.18	1.20	1.20
5* 1	.120	2.14	1.71	1.91	1.52	1.61	1.70	1.69
6* 1	.130	1.72	1.83	2.07	1.61	1.75	1.86	1.84
7* 1	.150	2.11	2.11	2.40	1.80	1.97	2.12	2.10
1* 2	.080	1.13	1.13	1.04	1.09	1.09	1.09	1.09
2* 2	.090	1.18	1.17	1.10	1.12	1.13	1.13	1.12
3* 2	.110	1.26	1.25	1.24	1.18	1.20	1.20	1.19
4* 2	.150	1.27	1.47	1.58	1.32	1.39	1.40	1.39
5* 2	.160	1.48	1.53	1.67	1.36	1.46	1.47	1.46
6* 2	.210	1.88	1.92	2.18	1.62	1.78	1.81	1.79
7* 2	.220	2.08	2.01	2.29	1.67	1.84	1.88	1.86
8* 2	.230	2.34	2.11	2.40	1.73	1.91	1.96	1.94
1* 4	.190	1.18	1.15	1.08	1.13	1.10	1.09	1.08
2* 4	.220	1.23	1.20	1.17	1.17	1.22	1.19	1.18
3* 4	.240	1.21	1.24	1.23	1.21	1.26	1.23	1.22
4* 4	.290	1.24	1.35	1.41	1.30	1.38	1.34	1.31
5* 4	.410	1.69	1.71	1.92	1.59	1.62	1.56	1.53
1* 6	.090	1.00	1.01	.84	1.02	1.01	1.01	1.01
2* 6	.120	1.04	1.03	.87	1.04	1.03	1.03	1.03
3* 6	.140	1.08	1.04	.89	1.06	1.04	1.04	1.04
4* 6	.150	1.00	1.04	.90	1.07	1.04	1.04	1.04
5* 6	.160	1.10	1.05	.91	1.08	1.05	1.06	1.06
6* 6	.210	1.13	1.09	.98	1.14	1.11	1.11	1.11
7* 6	.230	1.09	1.11	1.01	1.17	1.15	1.16	1.15
8* 6	.240	1.13	1.12	1.03	1.18	1.16	1.17	1.16
9* 6	.280	1.15	1.17	1.11	1.24	1.23	1.25	1.24
10* 6	.320	1.21	1.22	1.20	1.32	1.30	1.32	1.31
1* 7	.200	1.05	1.03	.87	1.03	1.04	1.03	1.02
2* 7	.230	1.07	1.04	.89	1.04	1.05	1.04	1.04
3* 7	.300	1.12	1.07	.95	1.07	1.09	1.07	1.06
4* 7	.350	1.12	1.10	1.00	1.09	1.14	1.11	1.10
5* 7	.390	1.16	1.13	1.04	1.11	1.18	1.14	1.13
6* 7	.450	1.19	1.17	1.11	1.15	1.24	1.19	1.18
7* 7	.530	1.27	1.24	1.22	1.21	1.30	1.24	1.23
8* 7	.590	1.22	1.30	1.32	1.26	1.37	1.30	1.28
9* 7	.690	1.40	1.41	1.49	1.35	1.38	1.31	1.29
10* 7	.720	1.36	1.44	1.54	1.38	1.39	1.32	1.31
11* 7	.900	1.46	1.69	1.90	1.59	1.47	1.38	1.38
12* 7	1.200	1.73	2.24	2.54	2.02	1.62	1.51	1.52

TABLE VII(continued)

No. n*s	d _e	E _{obs}	E ₁	E ₂	E ₃	E ₄	E ₅	E ₆
1* 8	.200	1.07	1.01	.84	1.03	1.01	1.01	1.01
2* 8	.220	1.05	1.02	.85	1.03	1.02	1.02	1.02
3* 8	.280	1.10	1.03	.87	1.06	1.04	1.04	1.04
4* 8	.370	1.08	1.06	.92	1.10	1.08	1.08	1.08
5* 8	.460	1.15	1.09	.98	1.15	1.11	1.12	1.12
6* 8	.600	1.24	1.15	1.09	1.26	1.20	1.21	1.22
7* 8	.670	1.20	1.19	1.15	1.32	1.25	1.27	1.27
8* 8	.770	1.32	1.26	1.26	1.42	1.30	1.32	1.33
1* 9	.290	1.07	1.06	.92	1.09	1.07	1.08	1.07
2* 9	.350	1.12	1.09	.97	1.13	1.12	1.13	1.12
3* 9	.450	1.15	1.15	1.07	1.21	1.20	1.22	1.20
4* 9	.530	1.20	1.21	1.17	1.29	1.28	1.32	1.29
5* 9	.620	1.26	1.28	1.30	1.39	1.34	1.39	1.35
1*10	.230	1.07	1.03	.86	1.04	1.03	1.03	1.03
2*10	.330	1.09	1.06	.92	1.09	1.08	1.08	1.08
3*10	.430	1.15	1.10	1.00	1.15	1.14	1.14	1.14
4*10	.490	1.18	1.13	1.05	1.20	1.19	1.19	1.19
5*10	.510	1.15	1.14	1.07	1.21	1.21	1.21	1.20
6*10	.580	1.21	1.19	1.14	1.27	1.24	1.24	1.24
7*10	.630	1.20	1.22	1.20	1.32	1.28	1.29	1.29
1*11	.170	1.07	1.05	.91	1.07	1.07	1.06	1.06
2*11	.240	1.12	1.11	1.00	1.13	1.15	1.14	1.13
3*11	.290	1.14	1.16	1.09	1.19	1.22	1.22	1.19
4*11	.330	1.15	1.20	1.17	1.25	1.27	1.27	1.24
5*11	.380	1.24	1.27	1.28	1.32	1.31	1.31	1.27
1*12	.144	1.03	1.10	1.00	1.12	1.04	1.04	1.04
2*12	.224	1.25	1.26	1.26	1.28	1.17	1.17	1.17
3*12	.243	1.44	1.31	1.33	1.33	1.20	1.20	1.20
4*12	.280	1.61	1.41	1.49	1.43	1.38	1.38	1.38
1*13	.144	1.02	1.10	1.00	1.12	1.04	1.04	1.04
2*13	.226	1.30	1.26	1.26	1.29	1.19	1.19	1.19
3*13	.249	1.44	1.32	1.35	1.35	1.25	1.25	1.25
4*13	.268	1.61	1.37	1.43	1.40	1.29	1.28	1.29
1*14	.305	1.02	1.07	.94	1.12	1.03	1.03	1.04
2*14	.456	1.15	1.16	1.09	1.26	1.16	1.16	1.18
3*14	.559	1.36	1.24	1.22	1.38	1.25	1.25	1.29
1*15	.299	1.01	1.07	.95	1.12	1.04	1.04	1.05
2*15	.418	1.12	1.15	1.07	1.23	1.14	1.14	1.16
3*15	.518	1.38	1.23	1.20	1.36	1.26	1.26	1.30
1*16	.151	1.05	1.10	1.00	1.09	1.10	1.08	1.08
2*16	.206	1.18	1.19	1.15	1.17	1.22	1.19	1.17
3*16	.263	1.34	1.32	1.36	1.28	1.38	1.33	1.31
4*16	.260	1.34	1.31	1.35	1.27	1.37	1.33	1.31
1*17	.177	1.07	1.14	1.06	1.13	1.08	1.07	1.07

TABLE VII(continued)

No. n*s	d _e	E _{obs}	E ₁	E ₂	E ₃	E ₄	E ₅	E ₆
2*17	.233	1.24	1.24	1.23	1.23	1.30	1.27	1.25
3*17	.268	1.37	1.32	1.36	1.30	1.41	1.37	1.35
4*17	.267	1.35	1.32	1.35	1.29	1.40	1.36	1.34
1*18	.185	1.00	1.05	.91	1.04	1.02	1.01	1.01
2*18	.210	1.00	1.07	.93	1.06	1.05	1.04	1.04
3*18	.245	1.05	1.09	.98	1.08	1.08	1.06	1.06
4*18	.340	1.15	1.18	1.13	1.15	1.23	1.18	1.17
5*18	.355	1.20	1.20	1.16	1.17	1.26	1.21	1.20
1*19	.230	1.01	1.05	.91	1.07	1.06	1.05	1.06
2*19	.295	1.03	1.09	.97	1.11	1.19	1.18	1.18
3*19	.330	1.09	1.11	1.01	1.14	1.19	1.17	1.18
4*19	.350	1.12	1.12	1.04	1.16	1.21	1.20	1.21
5*19	.408	1.30	1.17	1.11	1.22	1.32	1.31	1.31
6*19	.425	1.32	1.19	1.14	1.23	1.38	1.36	1.36
1*20	.200	1.21	1.38	1.45	1.33	1.56	1.58	1.53
2*20	.250	1.48	1.60	1.76	1.51	1.71	1.73	1.69
3*20	.300	1.72	1.36	2.11	1.72	1.86	1.89	1.85
4*20	.350	2.00	2.17	2.47	1.97	2.01	2.05	2.02
1*21	.288	1.21	1.20	1.17	1.27	1.28	1.32	1.32
2*21	.413	1.50	1.42	1.51	1.54	1.40	1.46	1.47
3*21	.475	1.66	1.56	1.71	1.70	1.47	1.54	1.56
4*21	.537	1.82	1.72	1.93	1.89	1.55	1.63	1.66
5*21	.600	1.99	1.90	2.15	2.11	1.62	1.71	1.76
1*22	.400	1.27	1.35	1.39	1.48	1.36	1.39	1.39
2*22	.450	1.33	1.44	1.54	1.61	1.40	1.44	1.44
3*22	.500	1.41	1.54	1.69	1.75	1.45	1.49	1.50
4*22	.550	1.48	1.66	1.85	1.90	1.49	1.54	1.55
5*22	.590	1.54	1.76	1.98	2.02	1.52	1.58	1.60
1*23	.325	1.08	1.06	.92	1.11	1.07	1.08	1.08
2*23	.413	1.12	1.09	.99	1.18	1.14	1.15	1.15
3*23	.450	1.14	1.11	1.02	1.21	1.17	1.18	1.19
4*23	.544	1.18	1.17	1.11	1.31	1.23	1.25	1.26
5*23	.613	1.21	1.21	1.19	1.39	1.26	1.29	1.30
1*24	.200	1.02	1.01	.84	1.03	1.02	1.02	1.02
2*24	.225	1.03	1.02	.85	1.04	1.03	1.03	1.03
3*24	.288	1.05	1.03	.88	1.07	1.06	1.06	1.06
4*24	.350	1.07	1.05	.91	1.10	1.09	1.10	1.10
5*24	.467	1.11	1.10	.99	1.18	1.14	1.15	1.15
1*25	.300	1.10	1.05	.92	1.10	1.11	1.11	1.11
2*25	.325	1.12	1.07	.93	1.11	1.12	1.13	1.12
3*25	.350	1.13	1.08	.95	1.13	1.14	1.14	1.14
4*25	.375	1.14	1.09	.97	1.15	1.15	1.16	1.15
5*25	.400	1.15	1.10	1.00	1.17	1.16	1.17	1.16
6*25	.413	1.16	1.11	1.01	1.18	1.17	1.18	1.17
1*26	.257	1.04	1.09	.98	1.07	1.04	1.04	1.04

TABLE VII(continued)

No. n_s	d_e	E_{obs}	E_1	E_2	E_3	E_4	E_5	E_6
2*26	.280	1.05	1.11	1.01	1.08	1.05	1.06	1.06
3*26	.289	1.07	1.12	1.02	1.09	1.06	1.07	1.07
4*26	.327	1.11	1.15	1.08	1.11	1.09	1.11	1.10
5*26	.368	1.13	1.19	1.15	1.14	1.14	1.16	1.16
6*26	.438	1.24	1.27	1.28	1.20	1.24	1.29	1.27
1*27	.287	1.12	1.11	1.02	1.15	1.12	1.11	1.12
2*27	.322	1.13	1.14	1.07	1.19	1.18	1.16	1.17
3*27	.344	1.14	1.17	1.11	1.22	1.20	1.18	1.19
4*27	.380	1.24	1.20	1.17	1.27	1.27	1.26	1.27
5*27	.421	1.34	1.25	1.24	1.32	1.35	1.34	1.35
6*27	.470	1.53	1.31	1.34	1.40	1.49	1.47	1.49
1*28	.204	1.19	1.09	.98	1.14	1.16	1.17	1.16
2*28	.210	1.32	1.10	.99	1.15	1.26	1.28	1.25
1*29	.236	1.58	1.12	1.04	1.22	1.32	1.33	1.38
2*29	.245	1.55	1.13	1.05	1.24	1.34	1.35	1.40
1*30	.371	1.11	1.04	.89	1.08	1.13	1.14	1.13
2*30	.418	1.23	1.06	.92	1.10	1.19	1.20	1.19
3*30	.462	1.41	1.07	.94	1.12	1.27	1.29	1.28
4*30	.508	1.43	1.08	.97	1.14	1.30	1.33	1.32
5*30	.583	1.71	1.11	1.02	1.19	1.35	1.38	1.37
1*31	.379	1.10	1.04	.90	1.09	1.13	1.13	1.14
2*31	.414	1.24	1.05	.92	1.11	1.18	1.19	1.19
3*31	.438	1.31	1.06	.93	1.12	1.24	1.25	1.25
4*31	.501	1.11	1.08	.96	1.16	1.29	1.29	1.30
5*31	.538	1.50	1.10	.99	1.18	1.31	1.32	1.33
1*32	.301	1.29	1.09	.98	1.14	1.32	1.32	1.29
2*32	.314	1.32	1.10	1.00	1.15	1.34	1.35	1.31
1*33	.273	1.10	1.08	.95	1.09	1.12	1.13	1.10
2*33	.294	1.09	1.09	.98	1.10	1.13	1.14	1.11
3*33	.314	1.09	1.10	.99	1.11	1.14	1.15	1.12
1*36	.402	1.08	1.05	.91	1.12	1.12	1.12	1.11
2*36	.449	1.11	1.07	.94	1.15	1.14	1.14	1.13
3*36	.502	1.12	1.08	.97	1.18	1.16	1.17	1.16
1*37	.380	1.17	1.05	.90	1.10	1.09	1.09	1.09
2*37	.452	1.20	1.07	.94	1.14	1.16	1.17	1.17
3*37	.465	1.50	1.07	.94	1.14	1.17	1.18	1.18
4*37	.521	1.63	1.09	.98	1.18	1.21	1.22	1.22
5*37	.577	1.69	1.11	1.02	1.22	1.25	1.27	1.27
1*38	.337	1.06	1.05	.91	1.10	1.08	1.08	1.08
2*38	.371	1.11	1.06	.93	1.12	1.11	1.11	1.11
3*38	.421	1.15	1.08	.96	1.15	1.15	1.16	1.16
4*38	.500	1.20	1.11	1.02	1.22	1.23	1.25	1.25
1*39	.405	1.55	1.07	.95	1.16	1.18	1.18	1.21
2*39	.433	1.62	1.08	.97	1.18	1.20	1.20	1.23
3*39	.465	1.70	1.10	.99	1.21	1.21	1.22	1.25
4*39	.505	1.76	1.11	1.02	1.25	1.24	1.25	1.29

TABLE VII (continued)

No. n*s	d _e	E _{obs}	E ₁	E ₂	E ₃	E ₄	E ₅	E ₆
5*39	.589	1.80	1.16	1.09	1.33	1.30	1.31	1.36
1*40	.284	1.32	1.14	1.06	1.19	1.45	1.46	1.41
2*40	.301	1.52	1.16	1.09	1.21	1.50	1.51	1.46
1*41	.223	1.13	1.11	1.01	1.15	1.30	1.31	1.27
1*42	.230	1.54	1.12	1.03	1.22	1.34	1.35	1.40
2*42	.234	1.65	1.13	1.04	1.22	1.34	1.35	1.40
1*43	.325	1.11	1.13	1.04	1.31	1.23	1.23	1.32
1*44	.437	1.12	1.06	.93	1.13	1.13	1.14	1.14
1*45	.437	1.09	1.06	.92	1.11	1.09	1.08	1.09
2*45	.503	1.16	1.08	.96	1.15	1.14	1.13	1.15
3*45	.531	1.21	1.09	.98	1.16	1.17	1.16	1.18
4*45	.612	1.41	1.12	1.03	1.21	1.24	1.24	1.26
5*45	.665	1.61	1.14	1.07	1.25	1.29	1.28	1.31
1*46	.352	1.11	1.25	1.24	1.09	1.08	1.09	1.08
2*46	.376	1.11	1.28	1.29	1.11	1.10	1.12	1.10
3*46	.414	1.16	1.34	1.39	1.13	1.14	1.16	1.14
4*46	.437	1.23	1.38	1.45	1.15	1.16	1.19	1.16
5*46	.481	1.31	1.46	1.57	1.18	1.21	1.26	1.21
1*47	.193	1.14	1.13	1.05	1.20	1.23	1.18	1.24
2*47	.218	1.17	1.17	1.12	1.25	1.28	1.23	1.31
3*47	.244	1.23	1.22	1.19	1.32	1.34	1.28	1.37
4*47	.254	1.23	1.24	1.22	1.34	1.37	1.30	1.40
5*47	.285	1.41	1.30	1.32	1.43	1.44	1.36	1.49
1*48	.795	1.06	1.28	1.29	1.08	1.04	1.05	1.05
2*48	.951	1.12	1.40	1.47	1.12	1.07	1.09	1.09
3*48	1.016	1.14	1.45	1.56	1.13	1.09	1.12	1.12
1*49	.190	1.22	1.13	1.04	1.15	1.17	1.14	1.15
2*49	.218	1.23	1.17	1.11	1.20	1.22	1.19	1.20
3*49	.236	1.31	1.20	1.16	1.23	1.26	1.23	1.24
4*49	.264	1.38	1.25	1.25	1.29	1.32	1.28	1.30
5*49	.279	1.47	1.28	1.29	1.32	1.36	1.31	1.33

AVERAGE PERCENTAGE DEVIATION FOR CORRELATION 1 = 7.80
AVERAGE PERCENTAGE DEVIATION FOR CORRELATION 2 = 13.63
AVERAGE PERCENTAGE DEVIATION FOR CORRELATION 3 = 7.42
AVERAGE PERCENTAGE DEVIATION FOR CORRELATION 4 = 6.16
AVERAGE PERCENTAGE DEVIATION FOR CORRELATION 5 = 6.01
AVERAGE PERCENTAGE DEVIATION FOR CORRELATION 6 = 5.86

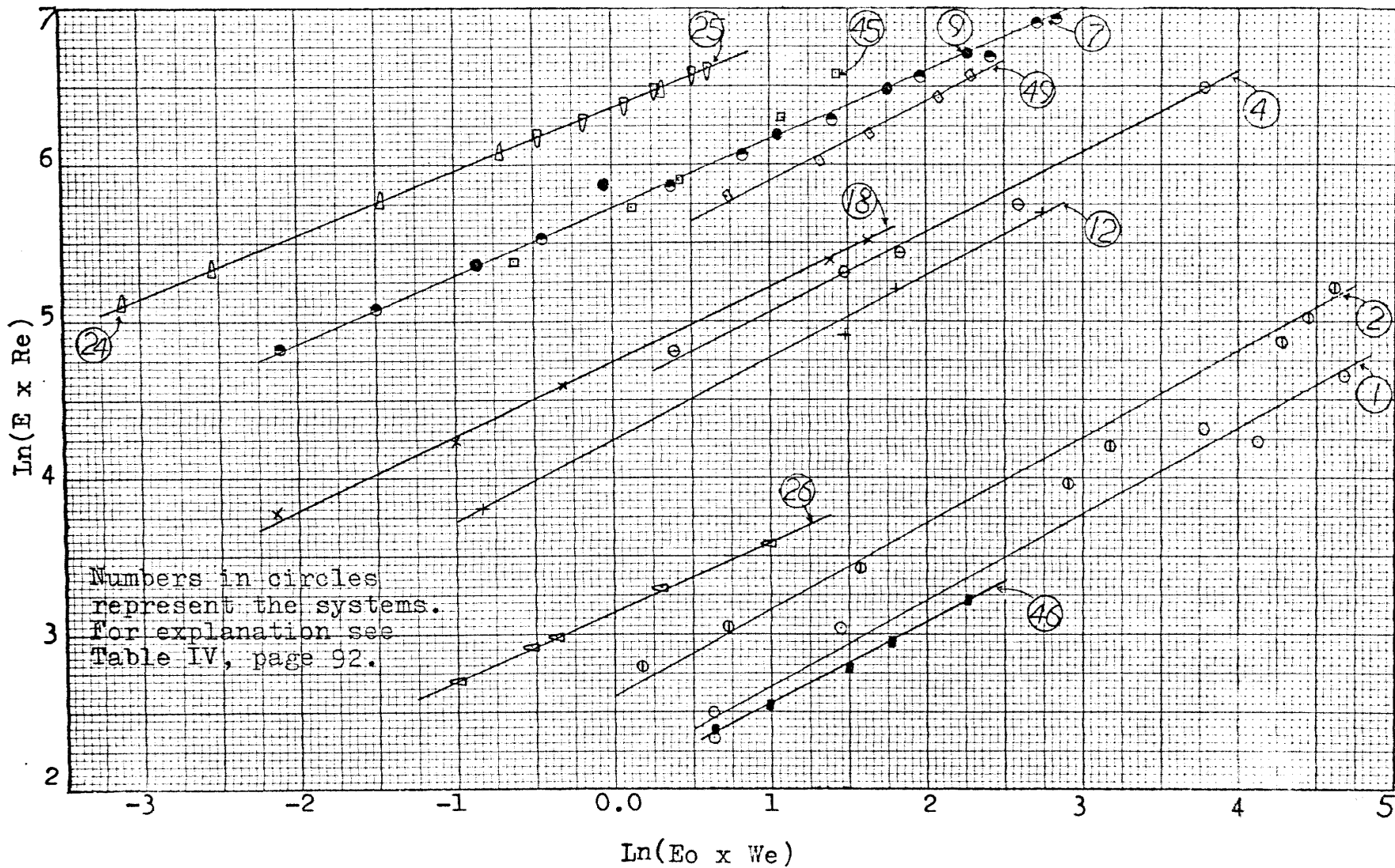


Figure 24. Plot of $\ln(E \cdot Re)$ versus $\ln(E_0 \cdot We)$

Appendix D.Nomenclature

- a = horizontal diameter, cm
 a' = $a/2$, cm
 A = surface area of drop, cm^2
 b = vertical diameter of drop, cm
 b' = $b/2$, cm
 C = $\frac{4}{3} \frac{\Delta\rho}{\rho_c} \frac{g d_e}{U_t^2}$, drag coefficient, dimensionless
 d_e = equivalent diameter of non-spherical particle, cm
 D = column diameter, cm
 e = $\sqrt{1-(1/E)^2}$, dimensionless
 E = a/b , eccentricity of drop, dimensionless
 E_o = $g \Delta\rho d_e^2 / \sigma_i$, Eotvos number, dimensionless
 f = a function
 Fr = $U_t^2 / g d_e$, Froude number, dimensionless
 g = acceleration due to gravity, 981 cm/sec^2
 j_d = $\frac{Sh}{Re Sc^{1/3}}$, j factor, dimensionless
 n = nth observation
 N = number of observations
 P = $\frac{\rho_c \sigma_i^3}{g \Delta\rho \mu_c^4}$, Physical properties group, dimensionless

$Re = d_e U_t \rho_c / \mu_c$, Reynolds number, dimensionless

s = system number

S = distance, cm

$Sc = \mu_c / \rho_c D_v$, Schmidt number, dimensionless

$Sh = k_c / d_l D_v$, Sherwood number, dimensionless

$We = \rho_c d_e U_t^2 / \gamma$, Weber number, dimensionless

D_v = molecular diffusivity, cm^2/sec

k_c = individual continuous phase mass transfer coefficient

Greek Letters

$\gamma = \sigma_i$, interfacial tension, dynes/cm

μ = viscosity, centipoises

ρ = density, gm/ml

$\Delta\rho = |\rho_c - \rho_d|$, density difference, gm/ml

$\sigma_i = \gamma$, interfacial tension, dynes/cm

Subscripts

c = continuous phase

d = dispersed phase

n = nth observation

l = characteristic length of the particle used

p = peak value

s = dimensions of a sphere of same volume as particle used

t = terminal value

1,2,3, = 1st, 2nd and 3rd observations or numbers

VIII. BIBLIOGRAPHY

1. Bond, W.N., and D.A. Newton, Phil. Mag. (7), 5 794 (1928)
2. Brown, G.G., et al., Unit Operations, p. 73, John Wiley & Sons Inc., New York (1960).
3. Efroymsen, M.A., Mathematical Methods for Digital Computers, ed. Ralston, A. and H.S. Wilfe, p. 191, John Wiley & Sons Inc., N.Y. (196).
4. Elzinga, E.R., and J.T. Banchemo, A.I.Ch.E. Journal, 7, 394(1961).
5. Garner, F.H., Trans. Inst. Chem. Engrs., (London), 28, 88(1950).
6. -----, and M. Tayeban, Anales de la Real Sociedad Espanola, de Fisica y Quimica, Serie B-Quimica, Tomo LVI (B), 479 (1960).
7. Harmathy, T.Z., A.I.Ch.E. Journal, 6 281 (1960).
8. Hu, S., and R.C. Kintner, A.I.Ch.E. Journal, 1 42 (1955).
9. Hughes, R.R., and E.R. Gilliland, Chem. Eng. Progr., 48, 497 (1952).
10. Johnson, A.I., and L. Braida, Can. J. Chem. Eng., 35, 165 (1957).
11. Keith, F.W., Jr., and A.N. Hixson, Ind. Eng. Chem., 47, 258 (1955).
12. Klee, A.J., Master Thesis, New York University, New York (1955).
13. -----, and R.E. Treybal, A.I.Ch.E. Journal, 2, 444 (1956).
14. Krishna, P.M., D. Venkateswarlu, and G.S.R. Narasimhamurty, J. of Chem. and Eng. Data, 4, 336 (1959).

15. Licht, William, and G.S.R. Narasimhamurty, A.I.Ch.E. Journal, 1, 366 (1955).
16. Null, H.R., and H.F. Johnson, *ibid.*, 4, 273 (1958).
17. Perry, J.H., Chemical Engineers' Handbook, IV ed., p. 3-70, McGraw Hill Book Co., New York (1963).
18. -----, *ibid.*, p. 5-59.
19. Strom, J.R., and R.G. Kintner, A.I.Ch.E. Journal, 4, 153 (1958).
20. Schroeder, R.R., and R.C. Kintner, *ibid.*, 11, 5 (1965).
21. Skelland, A.H.P., and A.R.H. Cornish, *ibid.*, 9 73 (1963).
22. Skelland, A.H.P., private communication to the author, University of Notre Dame, (February, 1965).
23. Treybal, R.E., Liquid Extraction, II ed., p. 182, McGraw Hill Book Co., New York (1963).
24. Wellek, R.M., private communication to the author, University of Missouri at Rolla, (1965).
25. Wu, H.C., Master Thesis, Master Thesis, Missouri School of Mines and Metallurgy, Rolla (1964).
26. Hodgman, C.D., Handbook of Chemistry and Physics, 43 rd. ed., p. 2211, The Chemical Rubber Publishing Co., Cleveland (1962).

IX. ACKNOWLEDGEMENTS

The author is deeply indebted to Dr. Robert M. Wellek, Assistant Professor in Chemical Engineering, who suggested this investigation and served as research advisor. His help, guidance and encouragement are sincerely appreciated. The author would also like to express his thanks to Dr. D.S. Wulfman, Assistant Professor in Chemistry, for his suggestion to use polaroids in photographing liquid droplets, and the Physics Department for loaning the polaroid sheets. The author is also thankful to Dr. M.R. Strunk, Chairman Department of Chemical Engineering, for his encouragement on various occasions.

The author gratefully acknowledges the following: Dr. A.H.P. Skelland who furnished additional eccentricity data; The Department of Chemical Engineering, Illinois Institute of Technology who donated the glass column used in this study; and Phillips Petroleum Company and Dow Chemical Company who supplied several of the solvents.

The author appreciates the graduate assistantship which enabled him to study at University of Missouri at Rolla.

X. VITA

The author was born on January 1, 1940, in Allahabad, India. He attended high school in Allahabad, graduating in 1953. After high school, the author attended the University of Allahabad, Allahabad, graduating in 1958 with a degree of Bachelor of Science. In 1958, the author joined Banaras Hindu University, Banaras, India and received a degree of Bachelor of Science in Chemical Engineering in 1962.

In September 1963 the author enrolled at University of Missouri at Rolla as a candidate for the Master of Science degree in Chemical Engineering.